1

Ambient Conditions Out- and Indoors

1.1 Overview

The role the ambient conditions have in building physics could be compared to the role loads have in structural engineering, the reason why the term 'ambient or environmental loads' is often used. Their knowledge is essential to make appropriate decisions when designing building envelopes and whole buildings. The components shaping the conditions out- and indoors are:

Outdoors		Indoors	
Air temperature	θ_e	Air temperature	θ_i
		Radiant temperature	θ_R
Relative humidity (RH)	ϕ_e	Relative humidity (RH)	ϕ_i
(Partial water) vapour pressure	p_e	(Partial water) vapour pressure	p_i
Solar radiation	E_S		
Under-cooling	q_{rL}		
Wind	v_w	Air speed	v
Rain and snow	g_r		
Air pressure	$P_{a,e}$	Air pressure	$P_{a,i}$

In what follows, all are discussed separately. Bear in mind though that the greater the difference between the out- and indoor temperature and relative humidity is, the stricter the envelope and HVAC performance requirements become. If not, maintaining thermally comfortable and environmentally healthy conditions indoors will among other things require more energy than acceptable.

Predicting the future climate outdoors remains a guess. Not only are most components not measured everywhere, but the future is never a copy of the past and does not obey the paradigm 'the longer the data chain available, the better the

Applied Building Physics: Ambient Conditions, Functional Demands, and Building Part Requirements, Third Edition. Hugo Hens.

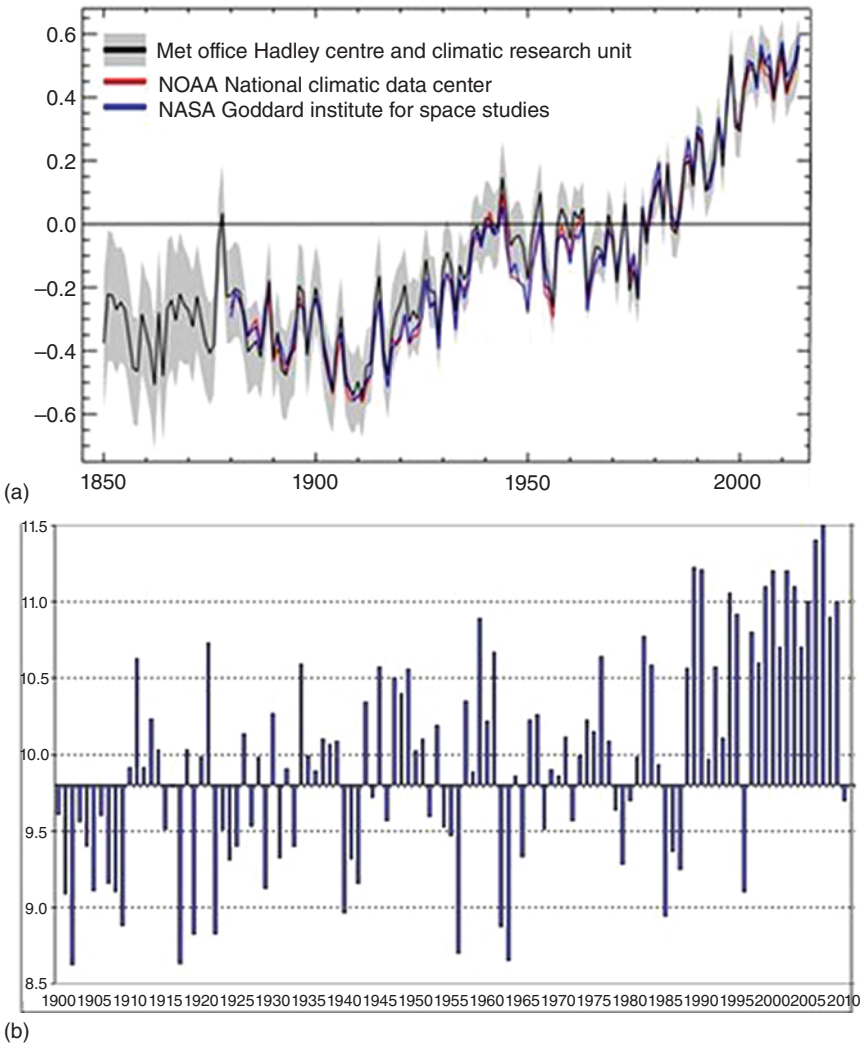

Figure 1.1 Global warming, (a) increase in the world's average annual temperature from 1850 to 2014; (b) the same for Uccle, Belgium.

forecast'. Moreover, global warming combined with the actual measures taken and future measures that will be taken to minimize the emission of global warming gasses, is loading any long-term prediction with uncertainty, see Figure 1.1.

A way to bypass that uncertainty is by using reference values and reference years for any performance check requiring climate data. Many of the facts and trends illustrating this in the book come from the weather station at Uccle, Belgium (50° 51′ north, 4° 21′ east). The large number of observations available there allowed to synthetize what happened over the last century.

1.2 Outdoors

1.2.1 In General

The geographic location is what largely determines the climate: northern or southern latitude, proximity of the sea, presence of a warm or cold sea current, and height above sea level. Of course, also microclimatic factors play. In city centres, the air temperature is on average 4–6 °C higher than at the countryside, while the relative humidity (RH) is lower and the solar radiation less intense, a reality called the urban heat island effect. To illustrate, Table 1.1 lists the monthly mean dry bulb temperatures measured at Uccle and Sint Joost for the period 1901–1930, both weather stations in the Brussels region, with the Uccle one situated in a green area and the Sint Joost one in the city centre.

From the annual down to the daily fluctuations, all are linked to the earth's elliptic orbit around the sun, the earth's inclination, the rotation around its axis and at its surface, more locally, the sequence of low- and high-pressure days. As a consequence, outside the equatorial band with its wet and dry seasons, each year sees a winter, springtime, summer and autumn passing. In addition, each 24 hours, day- and night-time alternate. In temperate and cold climates, high pressure brings warmth in summer and cold in winter, while low pressure cares for more moderate but often wet weather in summer and fresh but wet weather in winter. Anyhow, the last decennia, global warming is changing these patterns. New are more heat waves in summer, sequences of days showing excessive rain fall and warmer winters.

The data needed should focus on the annual cycle, the daily cycle and the daily averages. From a meteorological point of view, the 30-year averages, for the twentieth to twenty-first century 1901–1930, 1931–1960, 1961–1990, 1991–2020, 2021–2050, figure as the annual reference. Due to long-term climate changes induced by solar activity and global warming, the consequence of a still increasing imbalance between GW-gasses released and removed from the atmosphere, the trend to warmer, just mentioned, is real. Relocation of weather stations, more accurate measuring and the way averages are calculated also impact the data. Up to 1930, as daily mean was used the average between the daily minimum and maximum temperature logged by a minimum/maximum mercury thermometer. Today, the air temperature is logged each 10′ and the daily mean is calculated as the average of the 144 values so obtained.

Table 1.1 Monthly average dry bulb temperature at Uccle and Sint Joost, Brussels (°C).

Month	J	F	M	A	M	J	J	A	S	O	N	D
Uccle	2.7	3.1	5.5	8.2	12.8	14.9	16.8	16.4	14.0	10.0	5.2	3.7
Sint Joost	3.8	4.2	6.8	9.4	14.6	16.7	18.7	18.0	15.4	11.2	6.4	4.7

1.2.2 Air Temperature

Calculating the heating and cooling load and estimating related annual end energy use requires knowledge of the outside air temperature, while the loads so quantified fix the size and the investment in the HVAC installation and the energy use as annual cost. From day to day, the air temperature further impacts the heat, air, moisture stress building enclosures endure, while high hourly values increase overheating risk indoors. As imposed by the World Meteorological Organization (WMO), the measuring accuracy in the open field, 1.5 m above grade in a thermometer hut (Figure 1.2) should be ±0.5 °C. Table 1.2 gives the 30-year monthly averages for several weather stations across Europe and North America.

An annual average with one harmonic reflects the table data quite well, although two harmonics, the second on a half a year basis, do better:

$$\textit{Single harmonic}: \theta_e = \bar{\theta}_e + A_{1,1} \sin\left(\frac{2\pi t}{365.25}\right) + B_{1,1} \cos\left(\frac{2\pi t}{365.25}\right) \tag{1.1}$$

$$\textit{Two harmonics}: \begin{aligned} \theta_e = \bar{\theta}_e &+ A_{2,1} \sin\left(\frac{2\pi t}{365.25}\right) + B_{2,1} \cos\left(\frac{2\pi t}{365.25}\right) \\ &+ A_{2,2} \sin\left(\frac{4\pi t}{365.25}\right) + B_{2,2} \cos\left(\frac{4\pi t}{365.25}\right) \end{aligned} \tag{1.2}$$

In both $\bar{\theta}_e$ is the annual average and t time.

For three locations, the two harmonics gave as a result (°C, also see Figure 1.3):

	$\bar{\theta}_e$	$A_{2,1}$	$B_{2,1}$	$A_{2,2}$	$B_{2,2}$
Uccle	9.8	−2.4	−7.4	0.45	−0.1
Kiruna	−1.2	−4.2	−11.6	1.2	0.5
Catania	17.2	−4.1	−6.6	0.8	0.2

Figure 1.2 Thermometer hut.

Table 1.2 The thirty years based monthly mean air temperatures at several locations (°C).

Month location	J	F	M	A	M	J	J	A	S	O	N	D
Uccle (B)	2.7	3.1	5.5	8.2	12.8	14.9	16.8	16.4	14.0	10.0	5.2	3.7
Den Bilt (NL)	1.3	2.4	4.3	8.1	12.1	15.3	16.1	16.1	14.2	10.7	5.5	1.2
Aberdeen (UK)	2.5	2.7	4.5	6.8	9.0	12.1	13.7	13.3	11.9	9.3	5.3	3.7
Eskdale-muir (UK)	1.8	1.9	3.9	5.8	8.9	11.8	13.1	12.9	10.9	8.5	4.3	2.7
Kew (UK)	4.7	4.8	6.8	9.0	12.6	15.6	17.5	17.1	14.8	11.6	7.5	5.6
Kiruna (S)	−12.2	−12.4	−8.9	−3.5	2.7	9.2	12.9	10.5	5.1	−1.5	−6.8	−10.1
Malmö (S)	−0.5	−0.7	1.4	6.0	11.0	15.0	17.2	16.7	13.5	8.9	4.9	2.0
Västerås (S)	−4.1	−4.1	−1.4	4.1	10.1	14.6	17.2	15.8	11.3	6.3	1.9	−1.0
Lulea (S)	−11.4	−10.0	−5.6	−0.1	6.1	12.8	15.3	13.6	8.2	2.9	−4.0	−8.9
Oslo (N)	−4.2	−4.1	−0.2	4.6	10.8	15.0	16.5	15.2	10.8	6.1	0.8	−2.6
München (D)	−1.5	−0.4	3.4	8.1	11.9	15.6	17.5	16.7	13.9	8.8	3.6	−0.2
Potsdam (D)	−0.7	−0.3	3.5	8.0	13.1	16.6	18.1	17.5	13.8	9.2	4.1	0.9
Roma (I)	7.6	9.0	11.3	13.9	18.0	22.3	25.2	24.7	21.5	16.8	12.1	8.9
Catania (I)	10.0	10.4	12.0	14.0	18.0	22.0	25.2	25.6	23.2	18.4	15.2	11.6
Torino (I)	1.6	3.5	7.6	10.8	15.4	19.0	22.3	21.6	17.9	12.3	6.2	2.4
Bratislava (Sk)	−2.0	0.0	4.3	9.6	14.2	17.8	19.3	18.9	15.3	10.0	4.2	0.1
Copen-hagen (Dk)	−0.7	−0.8	1.8	5.7	11.1	15.1	16.2	16.0	12.7	9.0	4.7	1.1
Montreal	−9.9	−8.5	−2.4	5.7	13.1	18.4	21.1	19.5	14.6	8.5	1.8	−6.5
New York	0,6	2.2	6.1	11.7	17.2	22.2	25.0	24.4	20.0	13.9	8.9	3.3
Chicago	−5,6	−3,3	2,8	9,4	15,0	20,6	23,3	22,2	18,3	11,7	4,4	−2,8
Los Angeles	15,0	14,9	20,3	17,3	18,8	20,7	22,9	23,5	22,8	20,3	16,9	14,2

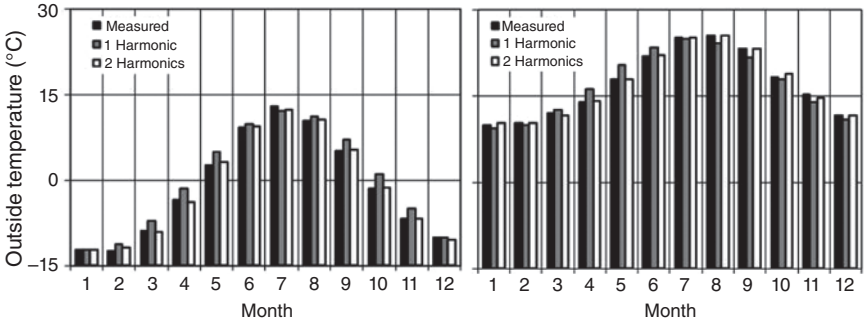

Figure 1.3 Air temperature: annual course, one and two harmonics; left: Kiruna, Sweden; right: Catania, Italy.

For Uccle the average difference between the monthly mean daily minimum and maximum temperature ($\theta_{e,max,day} - \theta_{e,min,day}$) during the period 1931–1960 is (°C):

J	F	M	A	M	J	J	A	S	O	N	D
5.6	6.6	7.9	9.3	10.7	10.8	10.6	10.1	9.8	8.0	6.2	5.2

A combination with the annual course gives (time in hours):

$$\theta_e = \bar{\theta}_e + \hat{\theta}_e \cos\left[\frac{2\pi(t-h_1)}{8766}\right] + \frac{1}{2}\left\{\Delta\bar{\theta}_{e,dag} + \Delta\hat{\theta}_{e,dag}\cos\left[\frac{2\pi(t-h_2)}{8766}\right]\right\}\sin\left[\frac{2\pi(t-h_3)}{24}\right] \quad (1.3)$$

with:

$\Delta\bar{\theta}_{e,dag}$ (°C)	$\Delta\hat{\theta}_{e,dag}$ (°C)	h_1 (h)	h_2 (h)	h_3 (h)
8.4	2.8	456	−42	8

The equation assumes that the daily values fluctuate harmonically, which is not the case. Instead, the gap between the minimum and maximum value swings considerably, without even a glue of being harmonic. To give an example, in Leuven, Belgium, the differences in January and July 1973 were random, with as averages 4.0 and 8.9 °C and as standard deviation 60% in January and 39% in July.

A question of course is whether the air temperatures recorded during the past decades reflect global warming. For that, data measured between 1997 and 2013 at the outskirts of Leuven were tabulated. Figure 1.4 shows the annual means and monthly minima and maxima. The least square line through the annual is:

$$\bar{\theta}_{e,ann} = 11.1 - 0.034 \cdot \text{year}$$

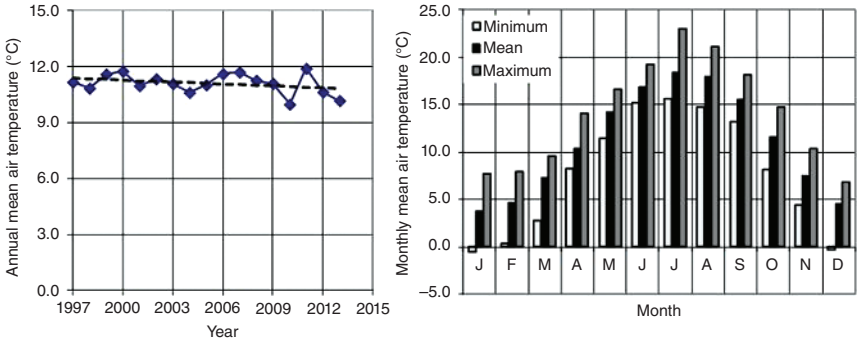

Figure 1.4 Leuven, Belgium, weather station: air temperatures between 1996 and 2013; left: the annual mean; right: the average, minimum, maximum, and monthly mean.

With on average 11.1 °C and a slightly negative slope, apparently, no increase appeared. Not so at Uccle, 30 km west of Leuven. There the overall average between 1901 and 1930 was 9.8 °C, i.e. 1.4 °C lower than measured from 1997 to 2013 in Leuven. From 1952 to 1971 the average in Uccle remained 9.8 °C but, since, the moving 20 years average is slowly increasing, with the highest values logged after 2001.

1.2.3 Solar Radiation

1.2.3.1 In General

The heat gains by solar radiation give less end energy needed for heating, though active cooling may loom as overheating might be the unintended consequence. Solar radiation further lifts the outside surface temperature of envelope assemblies, so enhancing drying and activating solar-driven vapour flow from rain-buffering outside finishes to inside. The concurring drop in RH may simultaneously increase the hygrothermal stress and strain in thin outside finishes.

The sun behaves as a 5762 K hot black body, ≈150 000 000 km away from the earth (=D_{se}). Through that distance, the rays reach the earth in parallel. Above the atmosphere, the solar spectrum coincides with the thin line in Figure 1.5, giving as irradiation:

$$E_{ST} = 5.67 \left(\frac{T_S}{100}\right)^4 \left(\frac{r_S}{D_{SE}}\right)^2 = 5.67 \times (57.64)^4 \times \left(\frac{0.695\ \ 10^6}{1.496\ \ 10^8}\right)^2 = 1332\,\mathrm{W/m^2} \tag{1.4}$$

with r_s the sun's radius in km.

This 1332 W/m^2 is called the average solar constant (E_{STo}), the mean radiation the earth should receive per m^2 perpendicular to the solar beam if without atmosphere, a flow, which is quite thin. Burning 1 l of fuel gives 4.4×10^7 J. Collecting so many Joules above the atmosphere per m^2 perpendicular to the moving solar beam will take nine hours, what explains why transforming solar energy into enough heat or electricity requires large collecting surfaces.

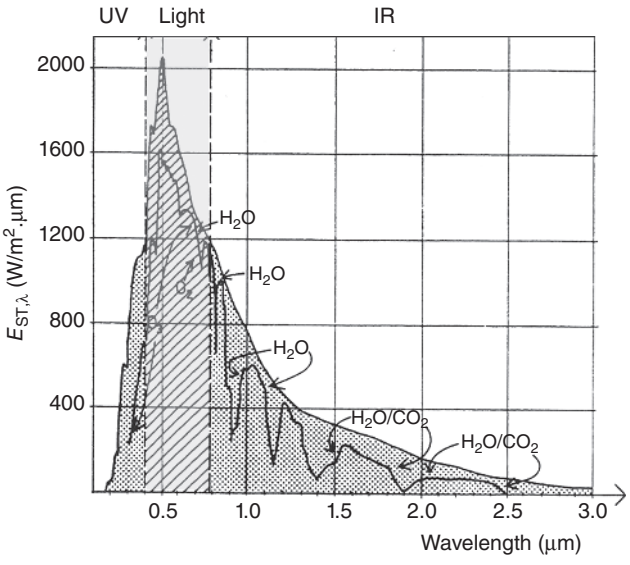

Figure 1.5 Solar spectrums before (upper line) and after passing the atmosphere (lower, up and down line).

A more exact calculation of the solar constant takes into account the annual variation in distance between earth and sun and the annual cycle in solar activity:

$$E_{STo} = 1373 \left\{ 1 + 0.03344 \cos \left[\frac{2\pi}{365.25} (d - 2.75) \right] \right\} (\mathrm{W/m^2}) \tag{1.5}$$

with d the number of days from midnight December 31/January 1. As the lower, up and down line along the spectrum in figure 1.5 shows, when crossing the atmosphere, gasses present, especially water vapour and CO_2, absorb part of the solar radiation, which definitely moderates what the earth surface receives.

To fix the sun's position on the sky, either the azimuth (a_s) and solar height (h_s) or the time angle (ω) and solar declination (δ), being the angle between both Tropics and the equator, can be used. The solar height touches 90° on December 21 when standing at zenith at the Tropic of Capricorn and on June 21 when standing at zenith at the Tropic of Cancer, see Figure 1.6. While the azimuth and solar height describe

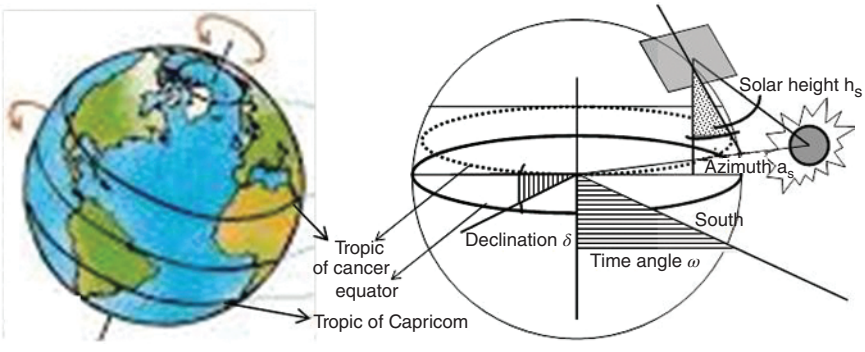

Figure 1.6 Solar angles.

the sun's movement locally on earth, the time angle and solar declination link it to the equator.

The time angle (ω) goes from 180° at midnight over 0° at noon to –180° next midnight. One hour so takes 15°. The solar declination (δ) in radians in turn equals:

$$\delta = \arcsin\left[-\sin\left(\frac{\pi}{180}23.45\right)\cos\left[\frac{2\pi}{365.25}(d+10)\right]\right] \tag{1.6}$$

where +23.45 and −23.45 are the latitudes of the tropic of Capricorn and the tropic of Cancer in degrees. The solar height in radians and the maximums ($h_{s,max}$) in degrees and rad follow from:

$$h_s = \max\left[0,\ \pi/2 - \arccos(\cos\phi\cos\delta\cos\omega + \sin\phi\sin\delta)\right] \tag{1.7}$$

$$\text{Degrees: } h_{s.max} = 90 - \phi(^\circ) + \delta(^\circ) \quad \text{Rad: } h_{s,max} = \pi/2 - \phi + \delta \tag{1.8}$$

with ϕ the latitude, positive in the northern, and negative in the southern hemisphere.

1.2.3.2 Beam Radiation

During the passage through the atmosphere, selective absorption by ozone, oxygen, hydrogen, carbon dioxide and methane muffle the solar rays, change their spectrum and scatter a part. The longer the distance so traversed, the larger these impacts, a fact the air factor m, the ratio between the distance the ray's traverse from the sun at solar height h_s to sea level and the distance they traverse from the sun in zenith to any location at and above sea level, accounts for (Figure 1.7).

For a location z km above sea level, the air factor so is:

$$m = \frac{L}{L_o} = \frac{1 - 0.1\,z}{\sin(h_s) + 0.15(h_s + 3.885)^{-1.253}} \text{ (solar height } h_s \text{ in rad)} \tag{1.9}$$

The beam radiation on a surface perpendicular to the rays consequently becomes:

$$E_{SD,n} = E_{STo}\exp(-m d_R T_{Atm})$$

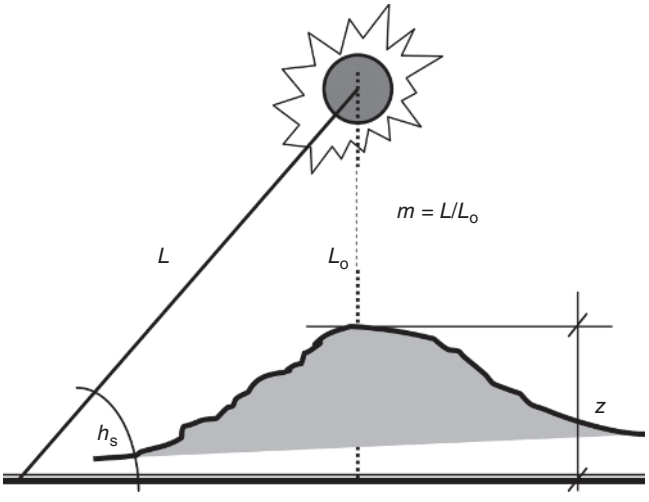

Figure 1.7 L distance traversed through the atmosphere from the sun at solar height h_s to sea level, L_o idem but now from the sun in zenith to a location at height z.

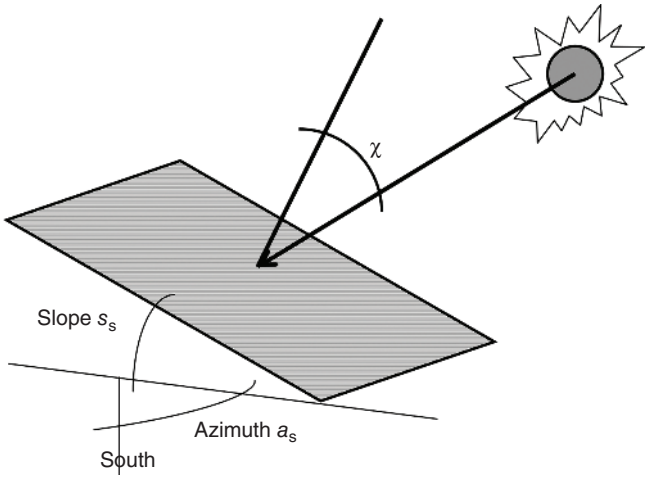

Figure 1.8 Direct radiation on a surface with slope s_s.

with T_{Atm} the atmospheric turbidity and d_R the optic factor, a measure for the scatter per meter traversed:

$$d_R = 1.4899 - 2.1099\cos(h_s) + 0.6322\cos(2h_s) + 0.0253\cos(3h_s) - 1.0022\sin(h_s) + 1.0077\sin(2h_s) - 0.2606\sin(3h_s) \quad (1.10)$$

On a clear day with average and minimal air pollution, the atmospheric turbidity (mo = 1 for January, mo = 12 for December) touches:

$$\textit{Average}: T_{Atm} = 3.372 + 3.037h_s - 0.296\cos(0.5236\,\text{mo})$$

$$\textit{Minimal}: T_{Atm} = 2.730 + 1.549h_s - 0.198\cos(0.5236\,\text{mo})$$

The beam radiation on a sloped surface, where the perpendicular to it forms an angle χ with the solar rays, now equals (Figure 1.8):

$$E_{SD,s} = \max(0, E_{SD,n}\cos\chi) \quad (0 \text{ before sunrise and after sunset}) \quad (1.11)$$

with:

$$\cos\chi = \sin\delta\,\sin\phi\,\cos s_s - \sin\delta\,\cos\phi\,\sin s_s\,\cos a_s + \cos\delta\,\cos\phi\,\cos s_s\,\cos\omega + \cos\delta\,\sin\phi\,\sin s_s\,\cos a_s\,\cos\omega + \cos\delta\,\sin s_s\,\sin a_s\,\sin\omega \quad (1.12)$$

In it, a_s is the azimuth (south 0°, east 90°, north 180°, west –90°) and s_s the slope of the surface (0° if horizontal, 90° ($\pi/2$) if vertical, 0 to 90° if sloped to, 0 to –90° ($-\pi/2$) if sloped away from the sun).

For a horizontal surface facing the sun, the formula becomes:

$$\cos\chi_h = \sin\delta\,\sin\phi + \cos\delta\,\cos\phi\,\cos\omega$$

For a south, west, north or east looking vertical surface facing the sun, it simplifies to:

$$\begin{aligned}
&\textit{South}: \cos\chi_{\text{v, south}} = -\sin\delta\cos\phi + \cos\delta\sin\phi\cos\omega\\
&\textit{West}: \cos\chi_{\text{v, west}} = -\cos\delta\sin\omega\\
&\textit{North}: \cos\chi_{\text{v, north}} = -\sin\delta\cos\phi - \cos\delta\sin\phi\cos\omega\\
&\textit{East}: \cos\chi_{\text{v, east}} = \cos\delta\sin\omega
\end{aligned}$$

With the beam radiation on a horizontal surface known ($E_{\text{SD,h}}$), the value on any sloped surface ($E_{\text{SD,s}}$) follows from:

$$E_{\text{SD,s}} = \max(0, E_{\text{SD,h}}\cos\chi_{\text{s}} / \cos\chi_{\text{h}}) \tag{1.13}$$

Beam radiation so looks predictable. The true unknown however is the atmospheric turbidity (T_{Atm}). Cloudiness, air pollution and RH, all intervene, but the impact is complex and varies from day to day.

1.2.3.3 Diffuse Radiation

Independently of whether the sky is blue or cloudy, the diffuse part of the solar radiation reaches the earth from sunrise to sunset. It looks as if the rays come from all directions. A simple model considers the sky as a uniformly radiating vault. Any surface, whose slope differs from horizontal, sees part of it. For the vault as black surface at constant temperature, each point on it has a same luminosity, giving as view factor with a surface:

$$F_{\text{s,sk}} = (1 + \cos s_{\text{s}})/2 \tag{1.14}$$

If $E_{\text{Sd,h}}$ is diffuse radiation on a horizontal surface, then on a sloped it equals:

$$E_{\text{Sd,s}} = E_{\text{Sd,h}}(1 + \cos s_{\text{s}})/2 \tag{1.15}$$

Closer to reality is the sky as a vault with highest luminosity at the solar disk and lowest at the horizon. For any point P on it characterized by its azimuth a_{P} and height h_{P}, related luminosity writes $L(a_{\text{P}},h_{\text{P}})$. The angle Γ between the perpendicular on a surface with slope s_{s} and the line from the surface's centre to that point P now equals:

$$\cos\Gamma = \sin s_{\text{s}}\ \cos h_{\text{P}}\ \cos(a_{\text{s}} - a_{\text{P}}) + \cos s_{\text{s}}\ \sin h_{\text{P}}$$

with $0 \le a_{\text{P}} \le 2\pi$ and $0 \le h_{\text{P}} \le \pi/2$. The diffuse radiation on the surface so becomes:

$$E_{\text{Sd,s}} = K_{\text{D}} \iint\limits_{a_{\text{P}},h_{\text{P}}} \left[L_{a_{\text{P}},h_{\text{P}}}\cos\ h_{\text{P}}\cos\Gamma\right] dh_{\text{P}}\, da_{\text{P}} \tag{1.16}$$

with:

$$K_{\text{D}} = 1 + 0.03344\cos\left[0.017202(d - 2.75)\right]$$

and:

$$L_{a_P,h_P} = L_{sd} \underbrace{\frac{[0.91 + 10\exp(-3\varepsilon) + 0.45\cos^2\varepsilon]\{1 - \exp[-0.32\ \mathrm{cosec}\ (h_P)]\}}{0.27385\left\{0.91 + 10\exp\left[-3\left(\frac{\pi}{2} - h_S\right)\right] + 0.45\sin^2 h_S\right\}}}_{f} \tag{1.17}$$

In it, L_{sd} is the luminosity at the solar disk and ε the angle between the line from the centre of the sloped surface to P and the perpendicular to the vault in P coinciding with the solar beam there:

$$\cos\varepsilon = \cos h_S\ \cos h_P\ \cos(a_S - a_P) + \sin h_S\ \cos h_P$$

Entering this formula and the multiplier f in the upgraded equation for diffuse radiation gives:

$$E_{Sd,s} = K_D L_{zenit} \iint_{a_P,h_P} \left[f \cos\ h_P \cos\ \Gamma\right] dh_P\ da_P$$

Luminosity at the solar disk now equals:

$$L_{sd} = 0.8785\,[h_s(^\circ)] - 0.01322[h_s(^\circ)]^2 + 0.003434[h_s(^\circ)]^3 + 0.44347 + 0.0364T_{Atm}$$

with T_{Atm} the atmospheric turbidity and h_s (°) the solar height. On a monthly basis, this set of formulas can be simplified to:

$$E_{Sd,s} = E_{Sd,h}\, f_{mo}(1 + \cos s_s)/2$$

with f_{mo} a multiplier correcting the monthly diffuse radiation calculated with the simple model for the other luminosity at the solar disk than at the horizon. Table 1.3 gives f_{mo} for Uccle.

Table 1.3 Uccle, multiplier f_{mo} for the total monthly diffuse radiation.

	Multiplier f_{mo}								
Slope↓Az→	**0, S**	**22.5**	**45**	**67.5**	**90, E,W**	**112.5**	**135**	**157.5**	**180, N**
0	1.00	1.00	1.00	1.00	1.00	1.00	1.00	1.00	1.00
22.5	1.03	1.03	1.02	1.01	1.00	0.99	0.98	0.97	0.96
45	1.05	1.04	1.03	1.01	0.99	0.96	0.94	0.92	0.92
67.5	1.06	1.05	1.03	0.99	0.94	0.90	0.86	0.84	0.83
90	1.06	1.04	1.00	0.94	0.87	0.81	0.76	0.73	0.71
112.5	0.98	0.97	0.92	0.85	0.76	0.68	0.63	0.60	0.60
135	0.80	0.78	0.74	0.67	0.59	0.53	0.49	0.47	0.47
157.5	0.58	0.56	0.51	0.48	0.46	0.43	0.41	0.40	0.34
180	0.00	0.00	0.00	0.00	0.00	0.00	0.00	0.00	0.00

1.2.3.4 Reflected Radiation

Any surface on earth reflects part of the solar radiation received. To calculate the intensity, the surroundings are considered acting as a horizontal plane with reflectivity 0.2, their albedo. Each surface so receives reflected radiation proportionally to its view factor with that plane (F_{se}):

$$E_{Sr,s} = 0.2\ (E_{SD,h} + E_{Sd,h})F_{se} = 0.2\,(E_{SD,h} + E_{Sd,h})(1 - \cos\, s_s)/2 \tag{1.18}$$

A horizontal surface facing the sky does not receive reflected radiation ($s_s = 0$), although it can in reality. A low-sloped roof for example may get reflected radiation from nearby higher buildings. Also, an albedo 0.2 is too simplistic. White snow gives much higher values.

1.2.3.5 Total Radiation

Beam, diffuse and reflected together fix the total solar a surface receives. The appendix contains tables with values for Uccle. Table 1.4 summarizes the average, minimum and maximum monthly totals measured on a horizontal surface there, together with related monthly mean cloudiness, calculated as one minus the ratio between the measured and total solar radiation on it under clear sky conditions.

Table 1.5 lists the monthly totals on a horizontal surface for several locations in Europe, while Figure 1.9 shows the annual totals. The ratio between least and most sunny location nears 2.

1.2.4 Clear Sky Long Wave Radiation

By cooling outer surfaces and the layers at the outside of the thermal insulation to below the air temperature, even to below the dewpoint outdoors, clear sky long wave radiation may induce extra heat losses. Related under-cooling so can turn the outdoor air into a moisture source causing condensation on the outer face of insulating glass and rime formation on EIFS insulated walls and on well-insulated tiled and slated roof pitches (Figure 1.10). Guilty is the long wave balance between the celestial

Table 1.4 Uccle, total solar radiation on a horizontal surface (MJ/(m^2 mo)), related cloudiness.

	J	F	M	A	M	J	J	A	S	O	N	D
Total solar radiation (1958–1975)												
Average	72	129	247	356	500	538	510	439	327	197	85	56
Min.	61	104	177	263	406	431	408	366	279	145	63	41
Max.	93	188	311	485	589	640	651	497	444	274	112	78
Related cloudiness (1958–1975)												
Average	0.47	0.44	0.42	0.42	0.36	0.35	0.38	0.38	0.34	0.39	0.49	0.50
Min.	0.55	0.55	0.58	0.57	0.48	0.48	0.51	0.48	0.44	0.55	0.62	0.63
Max.	0.31	0.19	0.27	0.20	0.25	0.22	0.21	0.30	0.11	0.15	0.33	0.30

Table 1.5 Monthly total solar irradiation on a horizontal surface in Europe (MJ/(m^2 mo)).

Month	J	F	M	A	M	J	J	A	S	O	N	D
Den Bilt (NL)	72	132	249	381	522	555	509	458	316	193	86	56
Eskdalemuir (UK)	55	112	209	345	458	490	445	370	244	143	70	39
Kew (UK)	67	115	244	355	496	516	501	434	311	182	88	54
Lulea (S)	6	52	182	358	528	612	589	418	211	80	14	1
Oslo (N)	44	110	268	441	616	689	624	490	391	153	57	27
Potsdam (D)	104	137	238	332	498	557	562	412	267	174	88	70
Roma (I)	182	247	404	521	670	700	750	654	498	343	205	166
Torino (I)	171	212	343	474	538	573	621	579	422	281	181	148
Bratislava (Sk)	94	159	300	464	597	635	624	544	389	233	101	72
Copenhagen (Dk)	54	114	244	407	579	622	576	479	308	159	67	38

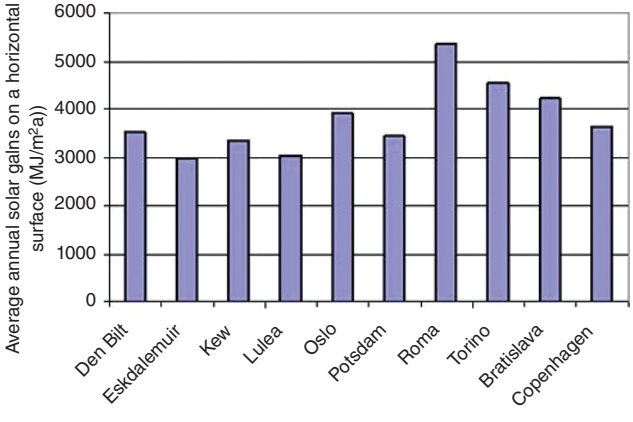

Figure 1.9 Annual solar irradiation on a horizontal surface.

Figure 1.10 Rime formation on a well-insulated pitched roof due to under-cooling.

vault, the sky, the terrestrial environment and the surface, with the sky as selective radiant surface, absorbing all but emitting only a fraction of the incident radiation.

Calculating starts by assuming the sky to be at air temperature while having an absorptivity 1, a reflectivity 0 and an emissivity given by (or, or with p_e in Pa, θ_e in °C):

Clear sky	**Cloudy sky**
(1) $\varepsilon_{L,\mathrm{sky},o} = 0.75 - 0.32 \cdot 10^{-0.051 p_e/1000}$	(4) $\varepsilon_{L,\,\mathrm{sky},\,o}(1 - 0.84c) + 0.84c$
(2) $\varepsilon_{L,\mathrm{sky},o} = 0.52 + 0.065\sqrt{p_e/1000}$	
(3) $\varepsilon_{L,\mathrm{sky},o} = 1.24\left(\dfrac{p_e/1000}{273.15 + \theta_e}\right)^{1/7}$	

As water vapour is a greenhouse gas, the clear sky three gives a decreasing value at higher air temperature but an increasing value at higher vapour pressure outdoors. In the cloudy sky one, c is cloudiness, 0 for a clear, 0.125–0.875 in steps of 0.125 for a hardly to very and 1 for a totally covered sky. According to Figure 1.11, the formulas (1) and (2) give different emissivities, while formula (3) suggests that (1) applies for lower, (2) for higher outside temperatures.

The black surface emittances of the surface ($M_{\mathrm{b,s}}$) and the terrestrial environment ($M_{\mathrm{b,t}}$) equal:

$$M_{\mathrm{b,s}} = \left[1 + \frac{\rho_{\mathrm{L,s}}}{\varepsilon_{\mathrm{L,s}}}(F_{\mathrm{s,t}} + F_{\mathrm{s,sky}})\right] M'_s - \frac{\rho_{\mathrm{L,s}}}{\varepsilon_{\mathrm{L,s}}}\left(F_{\mathrm{s,t}} M'_{\mathrm{t}} + F_{\mathrm{s,sky}} M'_{\mathrm{sky}}\right)$$

$$M_{\mathrm{b,t}} = \left[1 + \frac{\rho_{\mathrm{L,t}}}{\varepsilon_{\mathrm{L,t}}}(F_{\mathrm{t,s}} + F_{\mathrm{t,sky}})\right] M'_{\mathrm{t}} - \frac{\rho_{\mathrm{L,t}}}{\varepsilon_{\mathrm{L,t}}}\left(F_{\mathrm{t,s}} M'_{\mathrm{s}} + F_{\mathrm{t,sky}} M'_{\mathrm{sky}}\right)$$

In it, M'_{sky} is the radiosity of the sky and $F_{\mathrm{s,t}}, F_{\mathrm{s,sky}}$, etc. are the view factors between sky, terrestrial environment and surface. Since the first two surround the surface, $F_{\mathrm{s,t}} + F_{\mathrm{s,sky}} = 1$. The view factor between the terrestrial environment and the surface in turn is so small, that the second equation does not play. This makes $F_{\mathrm{t,sky}} = 1$, giving as radiosity of the sky:

$$M'_{\mathrm{sky}} = \varepsilon_{\mathrm{L,sky}} M_{b,\mathrm{sky},\theta_{\mathrm{e}}}$$

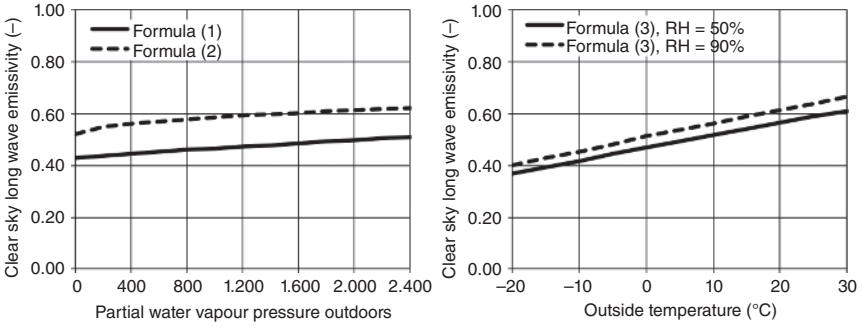

Figure 1.11 Clear sky emissivity; left: according to (1) and (2); right: to (3).

That changes the two black surface emittance equations into:

$$M_{\mathrm{b,s}} = \frac{1}{\varepsilon_{\mathrm{L,s}}} M'_{\mathrm{s}} - \frac{\rho_{\mathrm{L,s}}}{\varepsilon_{\mathrm{L,s}}} \left(F_{\mathrm{s,t}} M'_{\mathrm{t}} + F_{\mathrm{s,sky}} \varepsilon_{\mathrm{L,sky}} M_{\mathrm{b,sky},\theta_{\mathrm{e}}} \right) \tag{1.19}$$

$$M_{\mathrm{b,t}} = \frac{1}{\varepsilon_{\mathrm{L,t}}} \left(M'_{\mathrm{t}} - \rho_{\mathrm{L,t}} \varepsilon_{\mathrm{L,sky}} M_{\mathrm{b,sky},\theta_{\mathrm{e}}} \right) \tag{1.20}$$

The radiant heat flux at the surface so becomes:

$$q_{\mathrm{R}} = q_{\mathrm{Rs,t}} + q_{\mathrm{Rs,sky}} = \frac{\varepsilon_{\mathrm{L,s}}}{\rho_{\mathrm{L,s}}} \left(M_{\mathrm{b,s}} - M'_{\mathrm{s}} \right) = \varepsilon_{\mathrm{L,s}} F_{\mathrm{s,t}} (M_{b,\mathrm{s}} - \varepsilon_{\mathrm{L,t}} M_{\mathrm{b,t}}) + \varepsilon_{\mathrm{L,s}} F_{\mathrm{s,sky}} \left[M_{\mathrm{b,s}} - \left(\rho_{\mathrm{L,env}} \frac{F_{\mathrm{s,t}}}{F_{\mathrm{s,t}}} + 1 \right) \varepsilon_{\mathrm{L,sky}} M_{\mathrm{b,sky},\theta_{\mathrm{e}}} \right] \tag{1.21}$$

The assumption the terrestrial environment is a black surface at outside air temperature simplifies this equation to:

$$q_{\mathrm{R}} = \varepsilon_{\mathrm{L,s}} C_{\mathrm{b}} \left[(F_{\mathrm{s,t}} + F_{\mathrm{s,sky}}) \left(\frac{T_{\mathrm{se}}}{100} \right)^4 - (F_{\mathrm{s,t}} + F_{\mathrm{s,sky}} \varepsilon_{\mathrm{L,sky}}) \left(\frac{T_{\mathrm{e}}}{100} \right)^4 \right] \tag{1.22}$$

Making the sky a black surface too at temperature $\theta_{\mathrm{sk,\,e}} = \theta_{\mathrm{e}} - (23.8 - 0.2025\theta_{\mathrm{e}})(1 - 0.87c)$, gives:

$$q_{\mathrm{R}} = \varepsilon_{\mathrm{L,s}} C_{\mathrm{b}} \left[\begin{array}{l} (F_{\mathrm{s,t}} F_{\mathrm{Ts,t}} + F_{\mathrm{s,sky}} F_{\mathrm{Ts,sky}})(\theta_{\mathrm{se}} - \theta_{\mathrm{e}}) \\ \quad + (23.8 - 0.2025\theta_{e})(1 - 0.87c) F_{\mathrm{s,sky}} F_{\mathrm{Ts,sky}} \end{array} \right] \tag{1.23}$$

a result that fits with the equation for the radiant flux if the sky emissivity is set a little higher than assumed in Figure 1.11 right. Combining that result with the convective heat exchanged will quantify the importance of under-cooling:

$$q_{\mathrm{ce}} + q_{\mathrm{Re}} = [h_{\mathrm{ce}} + \varepsilon_{\mathrm{L,s}} C_{\mathrm{b}} (F_{\mathrm{s,t}} F_{\mathrm{Ts,t}} + F_{\mathrm{s,sky}} F_{\mathrm{Ts,sky}})](\theta_{\mathrm{se}} - \theta_{\mathrm{e}}) + \varepsilon_{\mathrm{L,s}} C_{\mathrm{b}} F_{\mathrm{s,sky}} F_{\mathrm{Ts,sky}} (23.8 - 0.2025\theta_{\mathrm{e}})(1 - 0.87c)$$

$$q_{\mathrm{T}} + q_{\mathrm{ce}} + q_{\mathrm{Re}} = 0$$

In it, q_{T} is the heat flux by transmission to or from the outer surface.

Figure 1.12 shows calculated data for a lightweight low-slope roof with $U = 0.2\,\mathrm{W/(m^2\,K)}$. Depending on wind speed and outside temperature, the outside surface temperature may drop quite a lot below the air temperature outdoors.

1.2.5 Relative Humidity (RH) and (Partial Water) Vapour Pressure

The RH and the vapour pressure have a decisive impact on the moisture tolerance of building enclosures and whole buildings. Table 1.6 summarizes the monthly means for several locations across Europe averaged over a 30-year period.

The RH hardly changes between winter and summer but vapour pressure does. On the other hand, large differences in RH but a fairly constant vapour pressure are often seen in temperate climates between day and night. A sudden rise in temperature lowers the RH, a sudden drop can push it to a misty 100%. During rainy weather, the wet bulb temperature closely follows the raindrop temperature. If equal to the air temperature, the RH will be near 100%. Also, the ambient has impact, with the

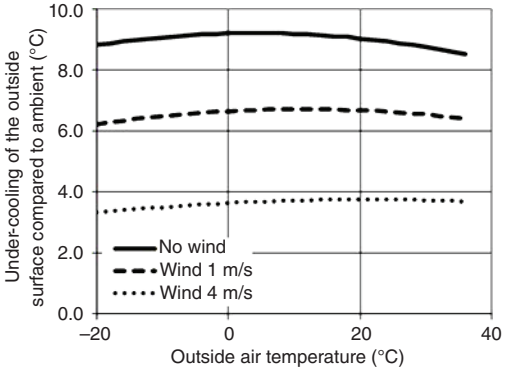

Figure 1.12 Lightweight low-sloped roof, $U = 0.2\,\mathrm{W/(m^2\,K)}$, membrane with $e_L = 0.9$: under-cooling represented by $\theta_e - \theta_{se}$.

Table 1.6 Monthly mean RH (%) and vapour pressure (Pa) for locations across Europe.

Loc. Month	J	F	M	A	M	J	J	A	S	O	N	D
Uccle (B)	89.6	89.0	84.0	78.5	77.8	78.9	79.9	79.8	84.2	88.3	91.2	92.7
	663	681	757	854	1151	1334	1529	1489	1346	1084	806	780
Aberdeen (UK)	81.5	80.3	74.9	72.3	75.0	78.5	74.1	79.1	80.6	81.6	78.1	77.1
	596	596	631	714	860	1107	1161	1207	1122	955	695	614
Catania (I)	66.5	72.4	68.8	69.8	71.2	70.0	62.0	68.6	69.4	69.6	68.5	65.9
	816	912	964	1114	1469	1849	1985	2252	1972	1471	1183	900
Den Bilt (NL)	86.1	82.1	76.0	75.9	72.9	72.7	77.1	78.9	80.7	84.4	85.5	86.8
	578	596	631	811	1028	1263	1411	1443	1306	1086	772	587
Kiruna (S)	83.0	82.0	77.0	71.0	64.0	61.0	68.0	72.0	77.0	81.0	85.0	85.0
	177	171	221	324	476	710	1011	914	676	436	292	219
Malmö (S)	87.0	86.0	83.0	76.0	73.0	74.0	78.0	77.0	82.0	85.0	87.0	89.0
	510	496	561	711	958	1262	1531	1464	1269	969	753	627
München (G)	83.7	81.9	76.8	72.3	74.9	76.8	74.2	76.1	79.2	82.9	83.5	85.7
	451	484	598	780	1043	1361	1483	1446	1267	938	660	515
Roma (I)	76.1	71.3	66.5	69.1	71.4	71.3	61.6	68.5	72.3	74.1	78.1	79.4
	794	764	816	1048	1400	1795	1881	2042	1776	1346	1124	874
Västerås (S)	84.0	82.0	74.0	66.0	62.0	65.0	69.0	74.0	81.0	83.0	86.0	86.0
	364	355	402	540	766	1081	1354	1328	1085	793	602	483

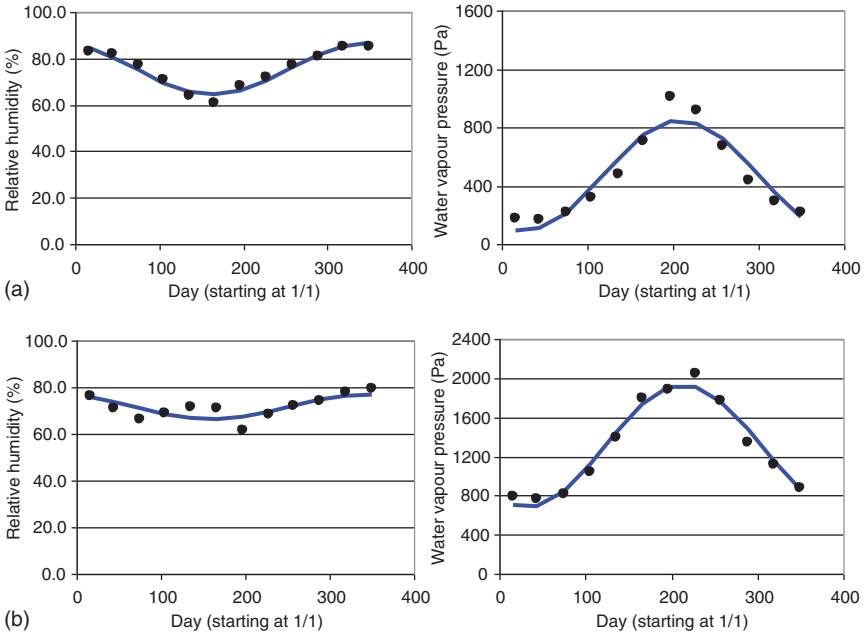

Figure 1.13 Monthly mean RH and vapour pressure in (a) Kiruna (Sweden), a cold climate, and (b) Rome (Italy), a rather warm climate, harmonic fit.

highest RHs and vapour pressures measured in forests and river valleys. Again, both annual variations can be written as a Fourier series with one harmonic:

$$\varphi_e = \bar{\varphi}_e + \hat{\varphi}_e \cos\left[\frac{2\pi(t-d)}{365.25}\right] \qquad p_e = \bar{p}_e + \hat{p}_e \cos\left[\frac{2\pi(t-d)}{365.25}\right] \tag{1.24}$$

with:

	Relative humidity (RH), %			Vapour pressure (p), Pa			Quality of the fit
	Average	Amplitude	d, days	Average	Amplitude	d, days	
Kiruna	75.5	11.1	346	469	380	209	RH±, p −
Roma	71.6	5.3	342	1305	627	214	RH−, p±

As Figure 1.13 illustrates, the deviation from the measured monthly averages can be significant.

1.2.6 Wind

1.2.6.1 Impact

Wind alters the hygrothermal response of building enclosures. Accelerated drying due to higher wind speeds shortens the first drying period. More wind lowers the sol-air temperature, counteracts under-cooling and increases the thermal transmittance of single glazing. It lifts uncontrolled air in- and exfiltration through

Figure 1.14 Sea-based wind turbines producing renewable electricity.

envelope leaks and favours air washing around poorly mounted insulation layers in cavities leaving open joints up and down and air layers in front and behind. The wind plus precipitation gives wind-driven rain, while higher wind speeds degrade comfort outdoors by exerting unpleasant dynamic forces, chilling people and complicating outer door handling. Positive anyhow is that more and more wind turbines deliver renewable electricity, so replace fossil-fuel power plants (Figure 1.14).

1.2.6.2 Wind Speed

Meteorologically, wind speed is seen as a horizontal vector, of which the amplitude and direction are measured in the open field at a height of 10 m. The average per 3″ is called the instantaneous, the average per 10′ the mean speed. Related spectrum includes several harmonics, while the vector's direction changes continuously.

Each local environment has impact on the amplitude and direction of the wind there. In small passages, venturi effects increase the speed, while eddies are formed along and windless zones behind buildings. Due to friction caused by terrain roughness, the wind speed felt increases from 0 m/s at ground level to a constant value in the 500 to 2000 m thick atmospheric boundary layer:

$$v_h = v_{10}\ K \ln(h/n) \tag{1.25}$$

In it, v_{10} is the average wind speed in flat, open terrain 10 m above ground level, v_h the average wind speed h meters above ground level, n the terrain roughness and K a friction factor:

Terrain upwind	K	n
Open see	0.128	0.0002
Coastal plain	0.166	0.005
Flat grass land, runaway area at airports	0.190	0.03
Farmland with low crops, spread farms	0.209	0.10
Farmland with high crops, vineyards	0.225	0.25
Open landscape with larger obstacles, forests	0.237	0.50
Old forests, homogeneous villages and cities	0.251	1.00
City centres with high-rises, industrial developments	≥0.265	≥2

Table 1.7 Uccle, ‰ of time wind comes from different directions (monthly means, 1931–1960).

	‰ of time											
Month → Orientation ↓	**J**	**F**	**M**	**A**	**M**	**J**	**J**	**A**	**S**	**O**	**N**	**D**
N	18	22	43	54	59	65	57	37	54	22	15	14
NNE	20	32	48	59	62	60	57	38	47	33	30	13
NE	41	65	79	103	85	72	64	44	67	65	58	47
ENE	54	65	68	68	75	56	40	38	62	63	56	56
E	56	61	48	53	72	45	34	41	63	63	64	41
ESE	28	32	30	28	39	25	26	25	34	38	32	29
SE	36	38	34	33	31	25	25	28	45	50	39	35
SSE	60	53	57	40	38	29	26	36	55	70	60	65
S	90	98	81	49	52	44	44	53	62	100	92	109
SSW	120	109	86	62	70	55	64	88	71	118	105	132
SW	163	130	113	105	92	103	131	152	104	124	142	147
WSW	125	115	100	97	92	100	120	145	103	85	119	125
W	92	73	79	78	71	95	109	121	94	77	89	91
WNW	50	49	54	59	49	74	68	64	55	46	51	46
NW	28	35	73	62	59	84	76	50	44	26	29	32
NNW	19	23	37	50	54	68	59	40	40	20	19	18

Table 1.7 and Figure 1.15 give the usual annual wind distribution over all orientations at Uccle.

Nearly half the year, wind in Uccle comes from west over southwest to south. Of course, other locations show other preferred directions.

1.2.6.3 Wind Pressure

That wind exerts a pressure when hitting an obstacle, follows from Bernoulli's law. Without friction, the sum of kinetic and potential energy in moving air must stay constant. Horizontally, the potential energy is linked to the pressure exerted. When an obstacle stops the wind, all kinetic energy turns into potential energy, giving as pressure (p_w):

$$p_w = \rho_a v_w^2/2 \,(\text{Pa}) \tag{1.26}$$

with ρ_a the air density ($\approx$1.2 kg/m^3) and v_w the wind velocity in m/s. As no obstacles are infinitely large, they only impede and redirect the wind. For buildings, this makes the pressure exerted different from the stop value, a fact the pressure coefficient (C_p) is accounting for:

$$p_w = \rho_a C_p v_w^2/2 \tag{1.27}$$

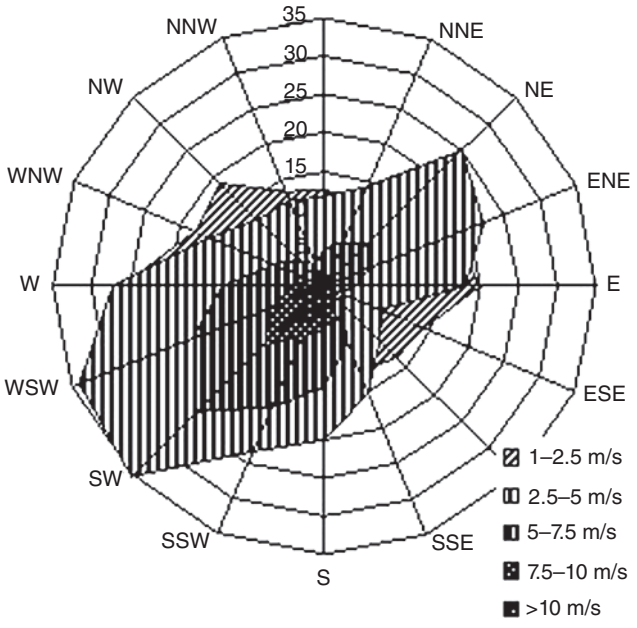

Figure 1.15 Typical wind rose for Uccle, Belgium.

Preferred as reference is the wind speed (v_w) measured at the nearest weather station, though others can be chosen. The pressure coefficients deduced from field measurement, wind tunnel experiments and CFD calculations depend on the reference chosen and the up- and downwind considered. The values building envelopes give vary from spot to spot. They are highest at the edges and upper corners, lowest on the façade's centre, positive at the windward side, negative at the leeward side and at sides more or less parallel to the wind direction, see Table 1.8.

1.2.7 Rain

1.2.7.1 Impact

Precipitation and wind-driven rain are among the largest moisture sources buildings must withstand. The term 'wind-driven' applies to the horizontal, the term 'precipitation' to the vertical rain component. While in windless weather the horizontal component is zero, at increasing wind velocity it becomes ever larger and may even win from the precipitation value. Horizontal and sloped outer faces collect rain under all circumstances, vertical faces only do when wind-driven, although run-off coming from sloped, sometimes horizontal surfaces may wet them. When rain buffering is the solution chosen to ensure a façade's rain-tightness, wind-driven rain and run-off will impact to some extend the energy used for heating and cooling.

1.2.7.2 Precipitation

Precipitation varies the way the wind does. Table 1.9 and Figure 1.16 give the mean duration in hours and the mean amounts per month at Uccle. As with wind, no

Table 1.8 Wind pressure coefficients for an exposed three floors high rectangular building with length-to-width ratio 2 to 1 (reference speed, the local at building height).

		Wind angle							
Location		**0**	**45**	**90**	**135**	**180**	**225**	**270**	**315**
Face 1 (Wind side)		0.5	0.25	−0.5	−0.8	−0.7	−0.8	−0.5	0.25
Face 2 (Rear side)		−0.7	−0.8	−0.5	0.25	0.5	0.25	−0.5	−0.8
Face 3 (Side wall)		−0.9	0.2	0.6	0.2	−0.9	−0.6	−0.35	−0.6
Face 4 (Side wall)		−0.9	−0.6	−0.35	−0.6	−0.9	0.2	0.6	0.2
Roof:									
Slope <10°	Wind side	−0.7	−0.7	−0.8	−0.7	−0.7	−0.7	−0.8	−0.7
	Rear side	−0.7	−0.7	−0.8	−0.7	−0.7	−0.7	−0.8	−0.7
	Average	−0.7	−0.7	−0.8	−0.7	−0.7	−0.7	−0.8	−0.7
Slope	Wind side	−0.7	−0.7	−0.7	−0.6	−0.5	−0.6	−0.7	−0.7
10 to 30°	Rear side	−0.5	−0.6	−0.7	−0.7	−0.7	−0.7	−0.7	−0.6
	Average	−0.6	−0.65	−0.7	−0.65	−0.6	−0.65	−0.7	−0.65
Slope	Wind side	0.25	0	−0.6	−0.9	−0.8	−0.9	−0.6	0
>30°	Rear side	−0.8	−0.9	−0.6	0	0.25	0	−0.6	−0.9
	Average	−0.28	−0.45	−0.6	−0.45	−0.28	−0.45	−0.6	−0.45

Table 1.9 Precipitation: duration and amounts per month, means for Uccle (1961–1970).

Precipitation↓	**J**	**F**	**M**	**A**	**M**	**J**	**J**	**A**	**S**	**O**	**N**	**D**
Duration (h)	53.6	57.3	51.9	51.5	41.9	36.0	42.9	38.8	36.5	52.5	67.3	72.7
Amount (l/m^2)	57.4	61.4	56.8	63.6	63.1	74.9	92.3	78.6	54.6	74.5	76.5	84.5

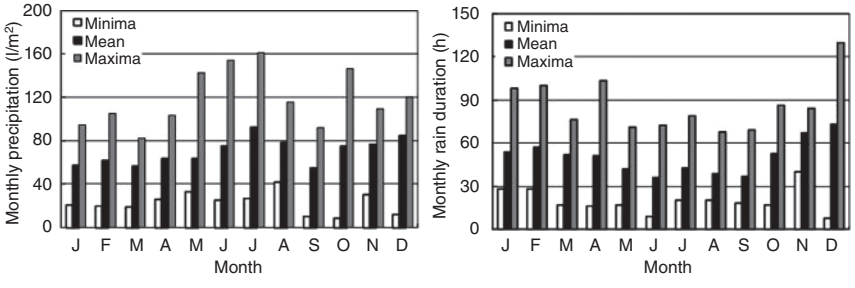

Figure 1.16 Precipitation: monthly amounts and duration for 1961–1970 at Uccle (averages, maxima and minima).

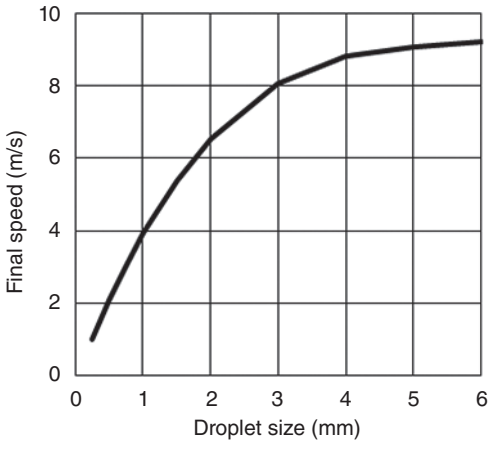

Figure 1.17 Final fall velocity of raindrops in windless weather.

annual cycle comes out, although slightly more rain is seen in summer, be it that global warming is actually moving that more to the winter months. The absolute maxima noted in Uccle were 4 l/m^2 in 1′, 15 l/m^2 in 10′ and 42.8 l/m^2 in one hour. Global warming is again changing this.

According to Best, rain showers have as droplet distribution ($F_{\mathrm{d,precip}}$):

$$F_{\mathrm{d,precip}} = 1 - \exp\left[-\left(\frac{d}{1.3 g_{\mathrm{r,h}}^{0.232}}\right)^{2.25}\right] \tag{1.28}$$

where $g_{\mathrm{r,h}}$ is the shower intensity in l/(m^2 h) and d the droplet size in m. When windless, the final fall velocity of raindrops is (see Figure 1.17):

$$v_\infty = -0.166033 + 4.91844d - 0.888016d^2 + 0.054888d^3 \ (d \text{ in mm}) \tag{1.29}$$

Depending on the mean droplet size, following terms are used to name precipitation:

Mean droplet size, mm	Kind of precipitation
0.25	Drizzle
0.50	Normal
0.75	Strong
1.00	Heavy
1.50	Downpour

1.2.7.3 Wind-driven Rain

The drag, wind provides, makes the droplet trajectories slant. How slant depends on their size, the wind vector's inclination compared to horizontal and the wind velocity

increase with height. A horizontally blowing constant wind keeps the trajectories straight, giving as wind-driven rain intensity ($g_{r,v}$, kg/(m^2 s)) in the open field:

$$g_{r,v} = 0.222 v_w g_{r,h}^{0.88} \tag{1.30}$$

with $g_{r,h}$ precipitation intensity in kg/(m^2 s). This equation is currently simplified to:

$$g_{r,v} = 0.2 v_w g_{r,h} \tag{1.31}$$

Wind velocities above 5 m/s so push the wind-driven rain intensity beyond the precipitation intensity. However, in the built environment, the equation falters. The intensity hitting a façade, in fact, depends on the horizontal rain intensity, the raindrop size distribution, the built volumes screening the building considered at the wind and the leeward side, the building's geometry, its orientation compared to the wind direction, where on the envelope the wind is hitting and how detailing there looks. Buildings in an open neighbourhood may so catch 40 times more wind-driven rain than buildings in a densely built environment.

The local amounts a facade receives link to the wind flow pattern around the building. For low-rises, the upper corners see most hits. When drizzling, high-rises catch the most at the highest floors, the higher edges and the upper corners, as the deposits measured on an 18-storeys building confirmed, see Table 1.10. The differences anyhow diminish at higher rain intensities and more wind

As formula to describe the wind-driven rain intensity impinging locally on enclosures is used:

$$g_{r,v} = \left(\underbrace{0.2 C_r v_w \cos \vartheta}_{} \right) g_{r,h} \tag{1.32}$$

In it, ϑ is the angle between the wind direction and the perpendicular to the face under consideration, while C_r is the wind-driven rain factor, a function of the kind of precipitation, the surroundings, the façade spot hit, local detailing, etc. On average, C_r varies from 0.25 to 2. The product above the bracket is called the 'catch ratio', representing the amount of wind-driven rain hitting a façade spot as fraction of the precipitation measured in the open field during related rain event. The formula is based on experimental evidence. Catch ratios measured on the south-west façade of

Table 1.10 Wind-driven rain on an 18-storey block of flats in Munich as measured by the Fraunhofer Institut für Bauphysik from May to November 1972.

Spot	Wind-driven rain, kg/m^2
Façade West, middle 3rd floor	29
Façade West, middle 9th floor	55
Façade West, middle 16th floor	65
Roof edge north	115
Roof edge south	130

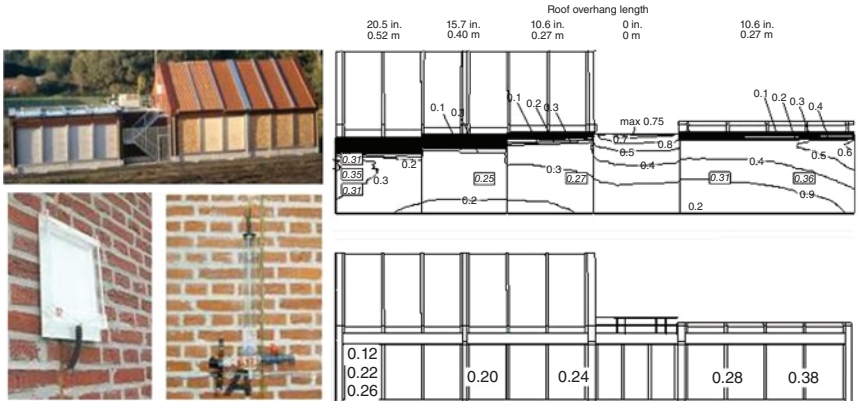

Figure 1.18 SW façade of a test building: calculated lines (middle) of equal catch ratio using CFD and droplet tracing compared to measured catches (bottom).

Figure 1.19 Average rain rose for Uccle.

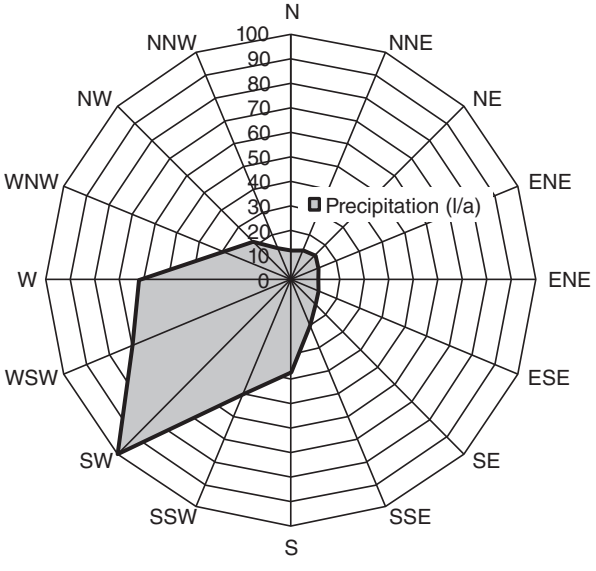

a test building were compared to what CFD-calculations for the wind field combined with droplet tracing gave, see Figure 1.18. Both fitted quite well.

In north-western Europe, wind-driven rain mainly comes from the south-west, see Figure 1.19 for Uccle. But strong winds and heavy precipitation hardly coincide. Between 1956 and 1970 the highest hourly means measured at Uccle were:

Precipitation, l/h	Mean wind speed, m/s
15	5.8
42	2.2

1.2.8 Microclimate Around Buildings

The direct environment around buildings has quite an impact as it affects solar shading, wind direction and velocity, the wind-driven rain patterns, the temperatures, etc. Even each part of a building enclosure experiences differences, depending on factors such as slope and orientation, located where, whether shaded and sheltered by protrusions and volumes above, etc. Together, all impact the damage tolerance of a building. This complexity, included the ever-changing character of the weather, forces to simplify through the use of design temperatures, reference days, reference years, etc. Of course, any evaluation so gives results, loaded with uncertainty.

1.2.9 Standardized Outside Climate Data

1.2.9.1 Design Temperature

In countries with a massive building tradition, the design temperature (θ_{ed},°C) for heating is either the lowest running two-day mean noted over a period of 20 years or the lowest daily mean noted over a period of 10 years. Many countries have maps giving these. In the USA and Canada, two countries with a timber-frame tradition, chosen can between an hourly value colder than either 99.6% or 99% of the 8790·T values, T being the period considered, actually 1986–2010. For Uccle, the two-days mean for the period 1971–1990 is −8 °C, the 99.6% and 99% hourly means from 1986 to 2010 −6.6 and −4.4 °C. Both are higher than −8 °C, mainly because 1986–2010 misses the cold winter of 1979. As global warming impacts these design values, each 10 or 20 years an upgrade is needed. Actually, the −8 °C became −7 °C. For cooling, the value used is the warmest hourly mean, exceeding either the 0.4% or 1% warmest value during the 1986–2010 period. This also holds for the wet bulb temperatures needed to fix the power (de)humidification requires.

1.2.9.1.1 Reference Years

The air temperature, the solar radiation, the long wave radiation and the wind are of decisive importance for the net heating and cooling demand but also for the overheating risk in summer. Therefore, several standard years were constructed: Hourly Thermal Reference Years, TRYs used in Building Energy Simulation tools (BES), an average TRY covering a series of successive years used to get the evolution of the annual net heating and net cooling demand, a warm TRY to evaluate overheating and quantify the annual net cooling load and a cold TRY to guess the annual net heating load. Average, warm and cold TRYs exist for several locations worldwide. Steady state calculations in turn use monthly averaged TRY's. The Belgian averaged cold and warm TRYs are based on the 1931–1960 averages and standard deviations, see Table 1.11. In it, cloudiness J stands for the ratio between the actual and the clear sky solar radiation on a horizontal surface.

The TRY advanced by the 2006 EPB legislation in Flanders, Belgium, combines the 1961–1990 monthly means for temperature, the total ($E_{ST,hor}$) and diffuse solar radiation ($E_{sd,hor}$) on a horizontal surface at Uccle, see Table 1.12. That global warming has impact, the column giving the monthly mean temperatures for the period 1991–2020 in Flanders is proving this.

Table 1.11 Monthly mean TRYs for Belgium (average, cold, warm).

Month	θ_e (°C)	$E_{ST,hor}$(W/m^2)	Wind (m/s)	RH (%)	P (Pa)	J (–)
Average year						
January	3.8	26.6	3.8	91	730	0.52
February	3.2	55.2	5.1	87	668	0.58
March	7.1	88.5	3.9	85	857	0.56
April	9.1	131.4	4.7	81	935	0.56
May	11.9	172.6	3.4	77	1072	0.59
June	16.7	216.9	3.2	80	1520	0.68
July	16.1	162.5	3.0	79	1445	0.53
August	17.1	158.0	3.5	83	1618	0.60
September	14.3	128.7	3.4	83	1352	0.67
October	11.0	64.9	3.6	91	1194	0.54
November	6.1	29.6	3.8	91	856	0.45
December	3.1	19.3	3.6	91	694	0.46
Cold year						
January	−3.9	33.2	4.1	86	379	0.65
February	−1.4	63.1	3.3	85	462	0.66
March	3.1	94.3	3.6	81	618	0.59
April	6.7	101.5	4.0	87	853	0.43
May	10.8	151.5	3.7	84	1087	0.51
June	14.2	178.7	3.1	79	1278	0.56
July	16.1	171.4	3.7	80	1463	0.55
August	15.9	136.7	3.5	86	1552	0.52
September	12.8	123.0	2.9	82	1211	0.64
October	7.5	53.9	3.3	90	932	0.44
November	4.2	40.2	4.6	88	725	0.62
December	0.2	25.3	3.2	90	558	0.61
Warm year						
January	6.8	25.3	5.2	87	859	0.50
February	7.6	55.4	4.4	89	928	0.58
March	8.5	109.4	3.5	85	942	0.69
April	12.3	130.7	3.0	86	1229	0.55
May	15.4	206.8	2.8	72	1258	0.70

(Continued)

Table 1.11 Monthly mean TRYs for Belgium (average, cold, warm). (Continued)

Month	θ_e (°C)	$E_{ST,hor}$ (W/m^2)	Wind (m/s)	RH (%)	P (Pa)	J (–)
June	18.8	235.2	3.1	74	1605	0.74
July	20.0	242.9	3.5	73	1706	0.79
August	19.9	181.7	2.9	74	1718	0.69
September	16.5	171.0	3.5	70	1313	0.89
October	13.8	86.2	2.6	86	1356	0.71
November	9.4	35.1	5.1	88	1036	0.54
December	7.4	15.4	5.3	87	895	0.37

Table 1.12 Energy performance legislation, reference year for Flanders, Belgium.

Month	θ_e (°C)	$\theta_{e,m}$ 1991–2020 (°C)	$E_{ST,hor}$ (MJ/m^2)	$E_{sd,hor}$ (MJ/m^2)
January	3.2	*3.7*	71.4	51.3
February	3.9	*4.2*	127.0	82.7
March	5.9	*7.1*	245.5	155.1
April	9.2	*10.4*	371.5	219.2
May	13.3	*13.8*	510.0	293.5
June	16.3	*16.7*	532.4	298.1
July	17.6	*18.7*	517.8	305.8
August	17.6	*18.4*	456.4	266.7
September	15.2	*15.2*	326.2	183.6
October	11.2	*11.3*	194.2	118.3
November	6.3	*7.2*	89.6	60.5
December	3.5	*4.4*	54.7	40.2

Remark: compared to the monthly mean reference temperatures imposed, the non-reference monthly means for 1991-2020 in the third column show the effect of a global warming.

1.2.9.2 Very Hot Summer, Very Cold Winter Day

Simpler than TRY's is taking a very hot summer and very cold winter day with probability once every 20 years, be it slightly changed to fit with being the last in a spell of equal days. This allows calculating harmonic responses. Table 1.13 lists the two for Uccle.

1.2.9.3 Moisture Reference Year

Starting at the end of the 1960s, calculation tools were developed to predict the moisture response of envelope assemblies. These require, among others, knowledge of the in- and outdoor conditions. The 1990s so saw the concept introduced of a 10 years valid moisture reference year, that over that period gave the highest wetness in an assembly. Of course, each moisture event should so require another year: wet

Table 1.13 Uccle: cold winter (declination −17.7°) and hot summer day (declination 17.7°).

	Very cold winter day			Very hot summer day		
Hour↓	Temp.°C	Direct sun, ⊥, W/m²	Diffuse sun, hor., W/m²	Temp.°C	Direct sun, ⊥, W/m²	Diffuse sun, hor., W/m²
0	−13.3	0	0	20.2	0	0
1	−13.6	0	0	19.8	0	0
2	−13.8	0	0	19.5	0	0
3	−14.2	0	0	19.0	0	0
4	−14.6	0	0	18.5	0	0
5	−15.0	0	0	18.0	136	6
6	−15.4	0	0	17.8	301	50
7	−15.5	0	0	17.8	440	87
8	−15.5	42	8	20.0	555	121
9	−14.9	336	47	22.0	645	146
10	−14.3	553	72	25.5	711	165
11	−13.1	636	89	28.0	752	180
12	−11.8	669	100	30.0	768	187
13	−11.7	656	105	30.8	759	188
14	−11.5	611	94	30.5	726	179
15	−11.9	564	72	30.0	669	165
16	−12.3	375	39	29.0	587	147
17	−12.8	47	11	27.8	480	121
18	−13.3	0	0	26.5	348	90
19	−13.7	0	0	25.5	192	49
20	−14.0	0	0	24.2	11	7
21	−14.5	0	0	23.0	0	0
22	−15.0	0	0	22.0	0	0
23	−15.1	0	0	20.5	0	0
24	−15.2	0	0	20.2	0	0

and windy for rain leakage, having a sunny summer regularly interrupted by rain spells for solar-driven vapour flow to the inside and cold and humid with a cloudy summer for interstitial condensation. Table 1.14 gives for some locations the year advanced for interstitial condensation.

For wind-driven rain, the alternative was using a moisture index. As more wetting and less drying worsens related tolerance both were combined. For that, in Canada, a normalized wetting (WI_{norm}) and drying (DI_{norm}) function is used:

$$WI_{norm} = \frac{WI - WI_{min}}{WI_{max} - WI_{min}} \qquad DI_{norm} = \frac{DI - DI_{min}}{DI_{max} - DI_{min}} \tag{1.33}$$

Table 1.14 Moisture reference years for interstitial condensation.

	Uccle			Rome			Copenhagen			Luleå		
Month	θ_e °C	p_e Pa	$E_{ST,h}$ W/m²	θ_e °C	p_e Pa	$E_{ST,h}$ W/m²	θ_e °C	p_e Pa	$E_{ST,h}$ W/m²	θ_e °C	p_e Pa	$E_{ST,h}$ W/m²
J	2.7	675	24.0	8.0	747	73.3	−0.1	569	18.2	−12.6	190	2.4
F	1.7	587	50.4	10.1	877	205.3	−0.4	507	53.1	−13.2	183	22.9
M	5.9	724	99.0	10.2	811	257.8	−0.3	476	83.4	−5.2	357	54.8
A	8.5	932	115.5	13.2	997	289.2	7.4	817	159.6	−2.4	415	109.8
M	12.6	1123	180.0	18.3	1323	243.6	12.0	1080	227.5	3.6	538	179.6
J	15.5	1374	215.0	22.3	1733	257.0	14.7	1355	229.4	10.8	894	234.4
J	14.9	1423	148.2	24.5	1976	271.1	15.3	1474	186.3	15.4	1365	203.9
A	16.2	1492	172.8	22.3	1747	224.0	15.1	1435	178.3	12.3	1144	122.6
S	13.5	1300	120.6	19.4	1524	187.8	12.6	1275	125.4	7.7	883	71.2
O	11.1	1097	102.1	17.1	1446	125.5	7.7	961	54.9	−2.4	430	28.4
N	4.0	716	40.1	11.5	1029	74.9	5.0	793	26.6	−4.1	401	4.3
D	4.8	783	15.6	9.6	907	51.2	1.1	614	15.9	−17.1	123	0.5

with WI the annual amount of wind-driven rain hitting a façade with given orientation at the location considered and DI equal to:

$$\mathrm{DI} = \sum_{h=1}^{k} \bar{x}_{\mathrm{sat}}(1 - \bar{\varphi})$$

where $\bar{x}_{\mathrm{sat}}$ is the hourly average vapour saturation ratio, $\bar{\varphi}$ the hourly mean RH and Σ the sum of all hourly means over a year at the location considered. The minimums $\mathrm{WI}_{\mathrm{min}}$ and $\mathrm{DI}_{\mathrm{min}}$ and maximums $\mathrm{WI}_{\mathrm{max}}$ and $\mathrm{DI}_{\mathrm{max}}$ represent the least and most severe year at Ottawa within a file of 30 successive years. For other locations, WI and DI relate to the third most severe year within that file. The moisture index then equals:

$$\mathrm{MI} = \sqrt{\mathrm{WI}_{\mathrm{norm}}^2 - (1 - \mathrm{DI}_{\mathrm{norm}})^2} \tag{1.34}$$

A first drawback is that only problems with wind-driven rain, not with interstitial condensation, are considered. A second is that solar radiation is completely overlooked, although drying primarily depends on the difference between the vapour saturation ratio on the outer face and in the outside air, a reality the sun dominates.

1.2.9.4 Equivalent Temperature for Condensation and Drying

In cold and temperate climates, interstitial condensation mainly deposits in interfaces at the cold side of the thermal insulation, typically because the thermal resistance from there to the outside is low. In these interfaces, the vapour saturation

pressure fluctuates with temperature. Due to their exponential relationship, higher temperatures have more impact than lower ones. So, on a monthly basis, the average saturation pressure there must differ from the value at the average interface temperature. It therefore makes sense to calculate the average saturation pressures in these interfaces beforehand and link them to a fictitious 'equivalent temperature outdoors for condensation and drying'. Experience learned this works well thanks to that low thermal resistance between the cold side of the thermal insulation and the outdoors.

To quantify, first, the sol-air temperature per month, per orientation and slope is calculated using hourly temperature, solar and long wave radiation data. Then, the hourly temperatures in the interface, where condensate deposits, follow from:

$$\theta_j = \theta_e^* + R_e^j \left(\theta_i - \theta_e^*\right)/R_a \tag{1.35}$$

with θ_i the temperature indoors, θ_e^* the sol-air temperature outdoors, R_e^j the thermal resistance from the interface with deposit to outdoors and R_a the thermal resistance of the assembly ambient to ambient. Next, the vapour saturation pressure in the interface is linked to these hourly temperatures, the average vapour saturation pressure per month calculated ($\bar{p}_{sat,j}$) and related 'fictitious' monthly mean interface temperature $\left(\bar{\theta}^*_{psat,j}\right)$, giving that average, fixed:

$$\bar{p}_{sat,j} = \frac{1}{T}\int_o^T p_{sat,j}\,dt \tag{1.36}$$

$$\bar{\theta}^*_{\bar{p}_{sat,j}} = F(\bar{p}_{sat,j}) \tag{1.37}$$

The monthly mean equivalent temperature outside for condensation and drying then follows from:

$$\bar{\theta}^*_{ce} = \frac{\bar{\theta}_{\bar{p}_{sat,j}} + \bar{\theta}_i \left(R_e^j/R_a\right)}{1 - R_e^j/R_a} \approx \frac{\bar{\theta}_{\bar{p}_{sat,j}}}{1 - R_e^j/R_a} \tag{1.38}$$

The sign ≈ tells the ratio R_e^j/R_a is small enough to neglect its product with the monthly mean inside temperature. This done for all months, the annual mean can be fixed and the first and second harmonic transposed in an annual amplitude, multiplied with a month-based a time function $C(t)$, see Table 1.15.

Table 1.16 gives the mean and amplitude at Uccle for a non-shaded, sun-radiated surface with shortwave absorptivity 1 and long wave emissivity 0.9.

Table 1.15 Uccle, $\theta^*_{ce} = \bar{\theta}^*_{ce} + \hat{\theta}^*_{ce}\ C(t)$, $C(t)$.

Month	$C(t)$	Month	$C(t)$	Month	$C(t)$	Month	$C(t)$
January	−0.98	April	−0.10	July	+1.00	October	−0.10
February	−0.85	May	+0.55	August	+0.85	November	−0.55
March	−0.50	June	+0.90	September	+0.55	December	−0.90

Table 1.16 Uccle, equivalent temperature for condensation and drying ($a_K = 1$, $e_L = 0.9$).

	Annual mean $\bar{\theta}^*_{ce}$ (°C)					Annual amplitude $\hat{\theta}^*_{ce}$ (°C)				
Slope↓ or →	**N**	**NW/NE**	**W/E**	**SW/SE**	**S**	**N**	**NW/NE**	**W/E**	**SW/SE**	**S**
0	14.4	14.4	14.4	14.4	14.4	12.6	12.6	12.6	12.6	12.6
15	13.7	13.9	14.4	14.7	14.8	12.4	12.5	12.6	12.7	12.7
30	12.9	13.4	14.2	14.9	16.0	11.7	12.0	12.3	12.4	12.4
45	12.2	12.8	13.9	14.7	14.9	10.9	11.3	11.6	12.0	11.8
60	11.9	12.6	13.7	14.6	14.7	9.8	10.6	11.2	11.3	11.1
75	11.8	12.4	13.5	14.3	14.6	9.3	10.0	10.7	10.6	10.3
90	12.1	12.6	13.6	14.2	14.4	9.1	9.5	9.9	9.7	9.5

Correcting for sun-radiated surfaces with shortwave absorptivity <1 is done by adapting the mean and the amplitude to:

$$\left[\bar{\theta}^*_{ce}\right] = \alpha_S \left(\bar{\theta}^*_{ce} - \bar{\theta}'_e\right) + \bar{\theta}'_e \tag{1.39}$$

$$\left[\hat{\theta}^*_{ce}\right] = \alpha_S \left(\hat{\theta}^*_{ce} - \hat{\theta}'_e\right) + \hat{\theta}'_e \tag{1.40}$$

In it, $\bar{\theta}'_e$ and $\hat{\theta}'_e$ are the annual mean and amplitude of the equivalent temperature for condensation and drying for a north-looking outer face with slope 45°, shortwave absorptivity 0 and long wave emissivity 0.9, for Uccle 8.5 and 7.1 °C. With long wave emissivity 0 or the surface permanently shaded, the annual mean air temperature and amplitude take over, for Uccle 9.8 and 6.9 °C. For non-shaded, sun-radiated surfaces with long wave emissivity between 0 and 0.9, a linear interpolation applies:

$$\bar{\theta}'_e = 8.5 + 1.3\left(\frac{0.9 - e_L}{0.9}\right) \qquad \hat{\theta}'_e = 7.1 - 0.2\left(\frac{0.9 - e_L}{0.9}\right) \tag{1.41}$$

The monthly mean equivalent temperature for condensation and drying for a non-shaded, sun-radiated surface so becomes:

$$\left[\theta^*_{ce}\right] = \left[\bar{\theta}^*_{ce}\right] + \left[\hat{\theta}^*_{ce}\right] C(t) \tag{1.42}$$

An estimate for sun-radiated surfaces shaded during part of the day demands an adaptation of Equation (1.40) to:

$$\left[\bar{\theta}^*_{ce}\right] = \alpha_K \left(\bar{\theta}^*_{ce} - \bar{\theta}'_e\right) \frac{E_{s,T,real}}{E_{s,T}} + \bar{\theta}'_e \qquad \left[\hat{\theta}^*_{ce}\right] = \alpha_K \left(\hat{\theta}^*_{ce} - \hat{\theta}'_e\right) \frac{E_{s,T,real}}{E_{s,T}} + \hat{\theta}'_e \tag{1.43}$$

with $E_{s,T}$ the total monthly solar radiation that the surface should receive if non-shaded, and $E_{s,T,real}$ the total monthly solar radiation it receives. Calculating the equivalent temperature for condensation and drying at other cold or temperate locations should proceed as explained.

1.2.9.5 Monthly Mean Vapour Pressure Outdoors

Calculating the yearly fluctuations of the monthly mean vapour pressure outdoors is done using the same time function $C(t)$:

$$p_e = \bar{p}_e + \hat{p}_e \; C(t) \tag{1.44}$$

with $\bar{p}_e$ and $\hat{p}_e$ the annual mean and amplitude, for Uccle 1042 and 430 Pa.

1.3 Indoors

1.3.1 In General

Building use presumes comfortable temperatures are maintained. Whether the RH requires control, depends on the climate and building use. Temperatures, RH and air pressure difference with outdoors also fix the ambient loads enclosures endure.

1.3.2 Air Temperature

1.3.2.1 In General

The air temperature affects thermal comfort as experienced, the end energy used for heating and cooling and the enclosure's moisture response. Standards focus on the operative temperature, see Table 1.17. However, in buildings, the air temperature is the parameter controlled, albeit a thermostat against a wall will sense a mix of the local air temperature and the wall's surface temperature, both impacted by the

Table 1.17 Operative temperatures needed according to DIN 4701 and EN 12831.

Building type	Room	Operative temperature	
		DIN 4701	EN 12831
Dwellings	Daytime and bedrooms	20	20
	Bathroom	24	24
Hospitals	Nursery	22	20
	Surgery, premature births	25	
Office buildings	All rooms	20	20
	Corridors, rest rooms	15	
Indoor swimming pool	Natatorium	28	
	Showers	24	
	Cabins	22	
Schools	Classroom		20
Department stores			20
Churches			15
Museum, galleries			16

little heat the sensor produces. Of course, in thermally well-insulated buildings, the operative and air temperature hardly differ.

1.3.2.2 Measured Data

1.3.2.2.1 Dwellings

Figure 1.20 shows the weekly mean air temperatures measured between 1972 and 2008 in 283 daytime rooms, 338 bedrooms and 37 bathrooms of poorly insulated homes as they depend on the average temperature outdoors during the test weeks. Between 2002 and 2005, extra data were collected in 39 well-insulated homes. Table 1.18 lists the regression constants and correlation coefficient found. In poorly insulated homes, the weekly means in the daytime rooms near the comfort value with some impact of the average temperature outdoors. In bed- and bathrooms instead, the weekly means are significantly lower and change strongly with the temperature outdoors. Are bathrooms heated when used, in bedrooms, heating is hardly on. Their indoor temperature reflects the balance between the gains from adjacent rooms, the losses to outside, the solar gains through the windows and the internal gains. Insulated, the conclusions differ. The daytime rooms remain well heated but

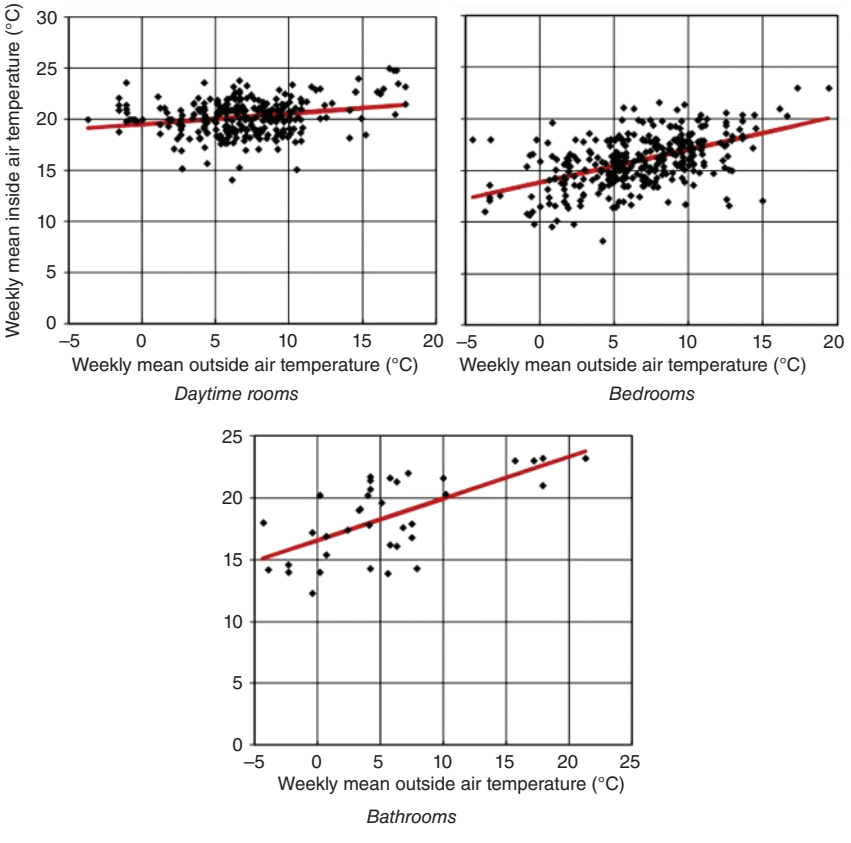

Figure 1.20 Poorly insulated dwellings: weekly mean air temperature in daytime rooms, bedrooms and the bathroom.

Table 1.18 Measured weekly mean air temperatures ($\bar{\theta}_i = a + b\bar{\theta}_e$).

	Weekly records	a (°C)	b (–)	Correlation
Poorly insulated homes				
Daytime rooms	283	19.5	0.11	0.06
Bedrooms	338	13.8	0.32	0.26
Bathrooms	37	16.5	0.34	0.43
Insulated homes				
Daytime rooms	39	19.3	0.22	0.89
Bedrooms	78	15.6	0.42	0.95
Bathrooms	39	19.9	0.20	0.82

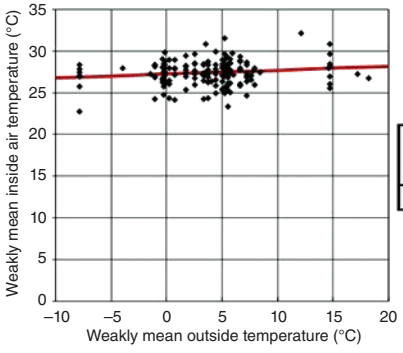

Number of weekly records	$\theta_i = a + b\theta_e$		Correlation coefficient
	a (°C)	b (–)	
162	27.3	0.045	0.02

Figure 1.21 Natatoriums: weekly mean temperatures indoors.

the bedrooms look warmer, probably due to the better insulation, although still, they remain intermittently or hardly heated. This clearly is a widespread habit. Bathrooms are warmer but still are impacted by the temperature outdoors.

1.3.2.2.2 Natatoriums

Figure 1.21 is linking 162 weekly mean air temperatures, logged in 16 natatoriums, to the corresponding weekly averages outdoors.

For the least square value and the correlation, see the table. On average, the measured values fit with what is preferred in natatoriums, 28 °C as operative temperature. Nonetheless, the lowest (22.2 °C) and highest value logged (32.2 °C) deviate substantially. Known is that leisure swimmers like higher, competition swimmers lower temperatures.

1.3.3 Relative Humidity (RH) and Vapour Pressure

1.3.3.1 In General

The RH and vapour pressure not only impact the indoor environmental quality, but they also play a key role when moisture tolerance is at stake. In temperate climates,

in dwellings, schools, shops, … the number of users and their activities impact both, while in museums, archives, cleanroom spaces, computer rooms, surgical and intensive care units the RH is controlled. This is also the case for dwellings in hot humid and in really cold climates.

1.3.3.2 Vapour Release Indoors

Tables 1.19–1.22 list data about the daily vapour release, the vapour release per activity, the hourly vapour release and the total vapour release per number of family members in dwellings. The means in Table 1.22 give as relation between vapour release and number of children:

$$G_{\mathrm{v,\,P}} = 3.2 + 2.8 n_{\mathrm{children}} \qquad r^2 = 0.28\ (\mathrm{kg/(day\,child)})$$

2.8 kg per child is a lot. More modest is 1 kg/(day child), see the last column of Table 1.22.

1.3.3.3 Measured Data

1.3.3.3.1 Dwellings

Figure 1.22 shows the weekly mean indoor to outdoor vapour pressure difference as measured between 1972 and 2008 in the 261 daytime, 315 bed- and 37 bathrooms of poorly insulated homes, depending on the average outside air temperature during the test weeks. Between 2002 and 2005, data also came from a long-term logging in 39 newly built, well-insulated homes.

Table 1.23 lists the least square lines, the 95% line and the correlation coefficients for both. For the hardly insulated, also a multiple regression between RH and air temperature in- and outdoors is included. In general, the difference between in and out decreases when warmer outdoors. Reasons are a more intense ventilation then and the hygric inertia of the building fabric, included all furniture and the furnishings, that dampens and shifts the annual amplitude indoors compared to outdoors. Most humid are the daytime rooms. The RH in all rooms anyhow decreases when these are warmer but when colder outdoors.

In insulated dwellings, the bed- and bathrooms remain quite close but the daytime rooms look dryer. Why, is unclear. Probably kitchen stove hoods became standard or the dwellings have less inhabitants, more volume per inhabitant and a better ventilation.

Analogous long-term measurements in the UK in 1065 living rooms and 916 bedrooms gave the results shown in Figure 1.23. The least-square regressions representing the means are:

$$\textit{Living rooms}\colon \Delta\bar{p}_{\mathrm{ie}} = 400 - 19.0\bar{\theta}_{\mathrm{e}}\,(\mathrm{Pa}) \qquad \textit{Bedrooms}\colon \Delta\bar{p}_{\mathrm{ie}} = 425 - 23.6\bar{\theta}_{\mathrm{e}}\,(\mathrm{Pa})$$

In Germany, measurements in 10 dwellings resulted in the straight lines, shown in Figure 1.24 with as least-square regression representing the mean:

$$\Delta\bar{p}_{\mathrm{ie}} = 328 - 13.7\bar{\theta}_{\mathrm{e}}$$

The indoor/outdoor vapour pressure differences so are lower when colder and higher when warmer outdoors than the UK ones. A why could be differences in venting habits: less window airing in Germany than in the UK when warmer outdoors?

Table 1.19 Dwellings, daily vapour release, depending on the number of family members.

Family members	Average water vapour release in kg/day		
	Low water usage[a)]	Average water usage[b)]	High water usage[c)]
1	3–4	6	9
2	4	6	11
3	4	9	12
4	5	10	14
5	6	11	15
6	7	12	16

a) Dwelling frequently unoccupied.
b) Families with children.
c) Teenage children, frequent showers, etc.

Table 1.20 Dwellings, vapour release linked to metabolism, activity and others.

	Activity	Release, g/h
Adults, metabolism	Sleeping	30
	At rest (depends on temperature)	33–70
	Light physical activity	50–120
	Moderate physical activity	120–200
	Heavy physical activity	200–470
Bathroom	Bath (15′)	60–700
	Shower (15′)	≤660
Kitchen	Breakfast preparation (4 people)	160–270
	Lunch preparation (4 people)	250–320
	Dinner preparation (4 people)	550–720
	Dish cleaning by hand	480
	Daily average release	100
Laundry drying	After dry spinning	50–500
	Starting from wet	100–1500
Plants (per pot)		5–20
Young trees		2000–4000
Full-grown trees		2×10^6–4×10^6

Table 1.21 Dwellings, vapour release during a weekday by a family of two and four.

Hour	Persons present	Release g/h				Sum
		Persons (g/h)	Cooking (g)	Hygiene (g)	Laundry (g)	
Family of 2, both working						
21–5	2	120		360		1440
6	2	120	240	720		1080
7	2	120	240			360
8–17	0					0
18	2	120				120
19–20	2	120	480			720
	Total	1680	960	1080		3720
Family of 4, father working, oldest child at school, mother and 1 child at home						
24–5	4	240				1440
6–7	4	240	960	1440		2880
8	2	120			120	240
9	1	60			180	240
10	1	60	720		180	960
11–12	2	120	600	120		960
13–14	2	120	480	120		840
15–17	2	120			240	480
18	4	240				240
19	4	240	480			720
20	4	240	480	240		960
21–22	4	240				480
23	4	240		240		480
	Total	4320	3720	2160	720	10920

Turning to the USA, temperature and RH have been logged in 60 homes, equally spread over three climate zones (Pacific northwest, a cold location in the northeast, and a hot and humid location in the southeast). Figure 1.25 gives the relation found between the moving monthly mean indoor/outdoor vapour pressure difference and the temperature outdoors. The figure underlines the dehumidifying effect of air conditioning. The least-square regressions for a running monthly average outside temperature below and above 19.5 °C give:

$$\leq 19\,^{\circ}\mathrm{C}\colon \Delta\bar{p}_{\mathrm{ie}} = 397 - 16.3\bar{\theta}_{\mathrm{e}}\ (r^2 = 0.86)\ >19\,^{\circ}\mathrm{C}\colon \Delta\bar{p}_{\mathrm{ie}} = 2807 - 140\bar{\theta}_{\mathrm{e}}\ (r^2 = 0.92)$$

Table 1.22 Daily vapour release in relation to the number of family members (several sources).

2 (no children)	3 (1 child)	4 (2 children)	>4 (more children)
8	12	14	>14 +1 kg/(day child)
	10		
7	20		
		14.6	
13.2	19.9	23.1	
	11.5		
	5–12		
	6–10.5		
4.3		13.7	
8.2	12.1	14.1	14.4
Mean: 8.14 kg/day	Mean: 11.9 kg/day	Mean: 15.9 kg/day	

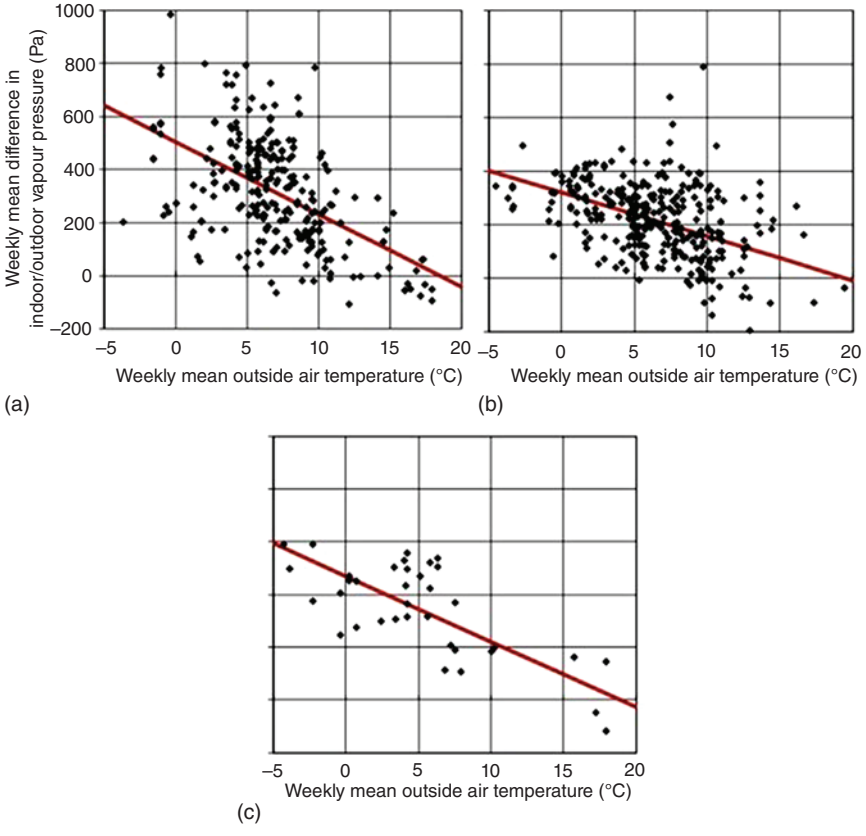

Figure 1.22 Poorly insulated homes: difference in weekly mean indoor to outdoor vapour pressure in daytime rooms (a), bedrooms (b) and bathrooms (c).

Table 1.23 Measured weekly indoor to outdoor vapour pressure differences and relative humidity.

	Number of records	$\Delta p_{ie} = a + b\theta_e$		Corr. r^2	$\phi_i = a + b\theta_i + c\theta_e$			Corr. r^2
		a, Pa	b, Pa/°C		a, %	b, %/°C	c. %/°C	
Poorly insulated homes								
Daytime rooms	261	**504**	**−27.2**	0.28	99.6	−2.6	−0.87	0.40
95% line		704	−27.2					
Bedrooms	351	**319**	**−16.3**	0.19	94.5	−3.4	−1.9	0.47
95% line		465	−16.3					
Bathrooms	37	**469**	**−24.9**	0.61	94.5	−2.5	−1.2	0.58
95% line		575	−24.9					
Insulated homes								
Daytime rooms	39	299	−12.4	0.53				
95% line		594	−18.0					
Bedrooms	39	261	−10.7	0.18				
95% line		497	−13.1					
Bathrooms	39	338	−11.3	0.64				
95% line		658	−16.1					

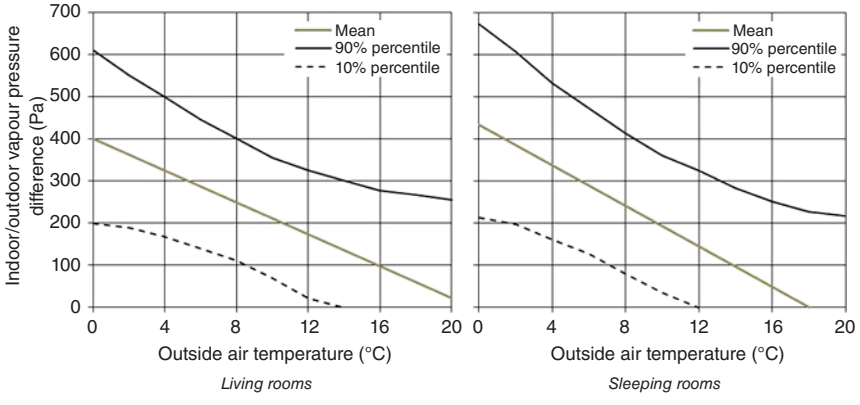

Figure 1.23 UK, 1065 living rooms (left) and 916 bedrooms (right): indoor to outdoor vapour-pressure difference: 10% percentile, 90% percentile and average in relation to the outside temperature.

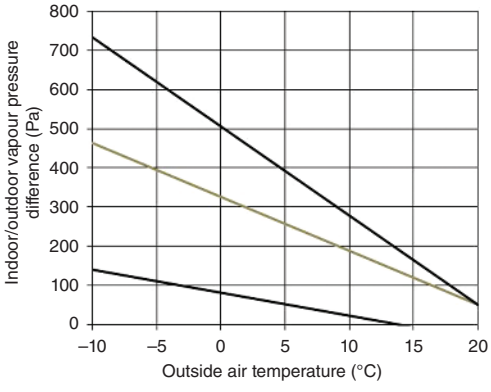

Figure 1.24 Germany, 10 homes, living room: lowest, highest, and mean indoor to outdoor vapour pressure difference line.

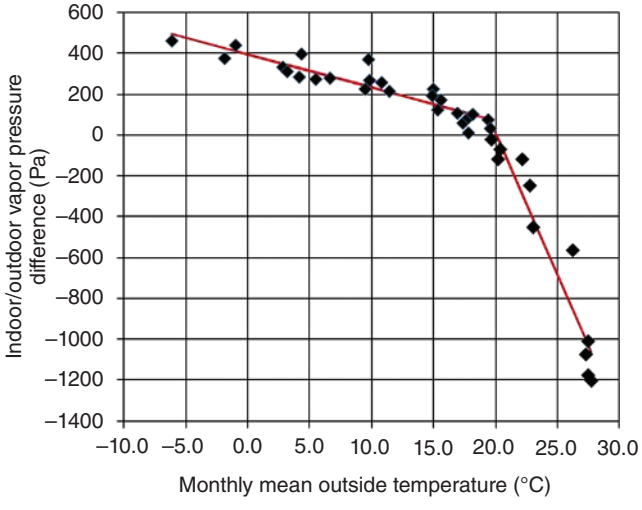

Figure 1.25 Monthly mean indoor to outdoor vapour pressure difference in relation to related outside temperature in three climate zones in the USA.

1.3.3.3.2 Natatoriums

Figure 1.26 shows 162 weekly mean indoor/outdoor vapour pressure difference logged in 16 natatoriums as function of the related weekly mean temperature outdoors. Table 1.24 gives the least-square regression and the correlation coefficients.

Again, the weekly means drop when warmer outdoors. Also notable is the large difference between the mean and the 95% line, indicating that natatoriums range from humid to very humid. Nevertheless, as Figure 1.27 shows, the RHs measured lay far below the wet swimmer's comfort zone. Main reason could be that the majority of these natatoriums had an enclosure not designed to tolerate the comfort RH, because, if the case, severe moisture damage could be expected. Keeping RH as low as measured anyhow demands so much ventilation that most natatoriums suffer from an inadmissible high and expensive end energy use for heating.

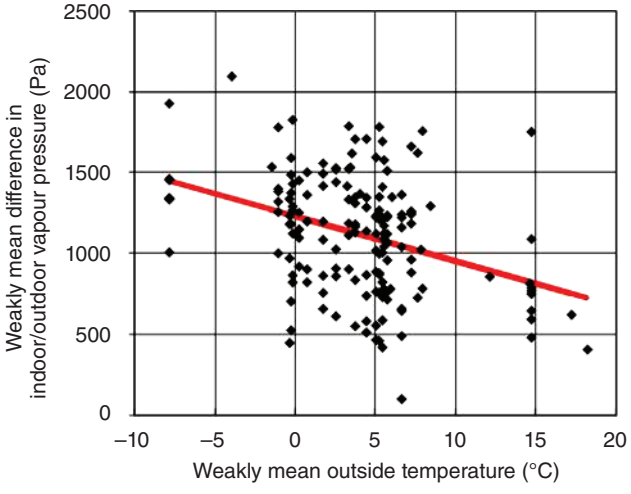

Figure 1.26 Natatoriums: weekly mean indoor to outdoor vapour pressure differences.

Table 1.24 Natatoriums, weekly mean indoor/outdoor vapour pressure difference and RH.

Number of records	Line	$\Delta p_{ie} = a + b\theta_e$		Correlation coefficient r^2	$\phi_i = a + b\theta_i + c\theta_e$			Correlation coefficient r^2
		a, Pa	b, Pa/°C		a,%	b, %/°C	c ,%/°C	
162	Mean	1229	–27.7	0.13	125	–2.8	0.36	0.17
	95%	1793	–27.7					

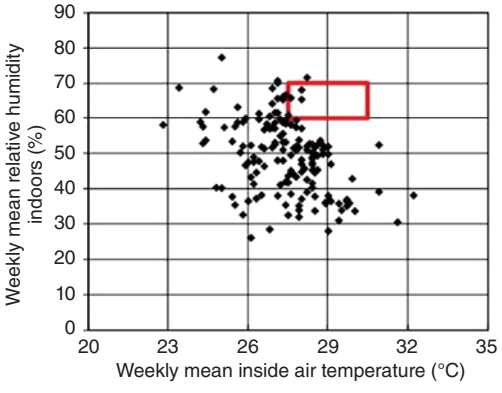

Figure 1.27 Natatoriums; left: weekly mean relative humidity indoors in relation to related temperature indoors with the rectangle fixing the comfort zone; right: dripping interstitial condensate humidifying the acoustical ceiling.

Table 1.25 Belgium, indoor climate classes ($\theta_{e,m}$: gliding monthly mean outdoor temperature).

	ICC	Upper pivot, Pa	Applies to buildings in which is fixed:
1	$\bar{\theta}_{e,m} < 0$ $\bar{\theta}_{e,m} \geq 0$	150 $150-8.9\bar{\theta}_{e,m}$	Vapour release only during short periods of time (dry storage rooms, sport arenas, garages, etc.)
2	$\bar{\theta}_{e,m} < 0$ $\bar{\theta}_{e,m} \geq 0$	540 $540-29\bar{\theta}_{e,m}$	Limited vapour release per m^3, ventilation appropriate (offices, schools, shops, large dwellings, apartments)
3	$\bar{\theta}_{e,m} < 0$ $\bar{\theta}_{e,m} \geq 0$	670 $670-29\bar{\theta}_{e,m}$	More vapour release per m^3, ventilation appropriate (small dwellings, hospitals, pubs, restaurants)
4	$\bar{\theta}_{e,m} < 0$ $\bar{\theta}_{e,m} \geq 0$	>670 $>670-29\bar{\theta}_{e,m}$	Much vapour released per m^3 (natatoriums, breweries, several industrial complexes, hydro-therapy spaces)

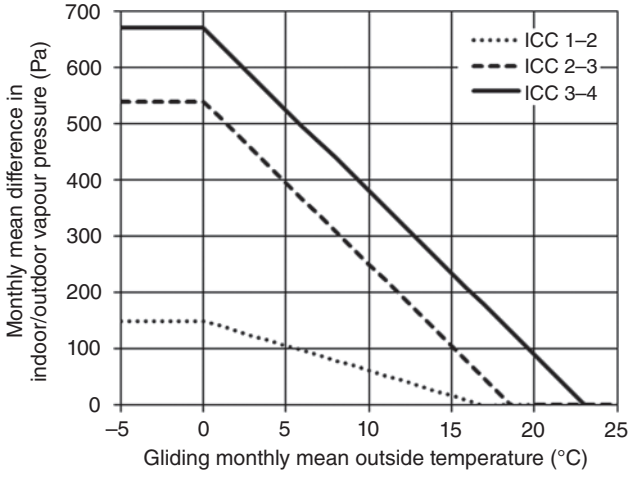

Figure 1.28 Belgium, pivots between the four indoor climate classes.

1.3.3.4 Indoor Climate Classes

The difference in indoor/outdoor vapour pressure is so important for moisture tolerance that buildings were grouped in indoor climate classes (ICC) with the difference between the two as pivot. Table 1.25 gives the ICCs as defined for Belgium, also see Figure 1.28.

The pivots handled reflect following situations:

Class 1/2 On a monthly basis, vapour diffusion does not give interstitial condensation in a continuously shaded, airtight low-slope roof without vapour retarder, composed of non-hygroscopic materials and covered with a vapour tight membrane

Class 2/3	On a monthly basis, vapour diffusion does not give accumulating condensate in a north-oriented, non-hygroscopic, airtight wall without vapour retarder at the inside, finished at the outside with a vapour-tight cladding
Class 3/4	On a monthly basis, vapour diffusion results in accumulating condensate in the reference roof of class 1/2, now sun-radiated

In indoor climate class 4 buildings, a correct heat, air, moisture design of the enclosure is crucial, while in climate class 1, 2 and 3 buildings, respecting simple design rules suffices. In the 1990s, the pivot lines have been recalculated using transient modelling. Main result was a shift of the pivot line between classes 3 and 4, see Table 1.26.

Other countries did a same exercise. Table 1.27 and Figure 1.29 left summarize the results for Finland and Estonia. To fix the pivot lines, data from 101 dwellings spread over both countries were used.

A Europe-wide adoption of the ICC concept came with the EN-ISO 13788. This standard distinguishes 5 classes with as pivots lines those given in Table 1.28 and the figure added.

When airflow-driven vapour movement intervenes, the classes as fixed lose usability. The concept in fact was developed to evaluate the slow condensation deposit with diffusion only as driving force, not the much faster built-up, what a convective vapour flow gives. Even ICC 1 buildings may experience problems then.

Table 1.26 Belgium, pivots between the ICC's recalculated (if <0, set 0).

Indoor climate class	Pivot (Pa)		Pivot (Pa)	
1–2	$\bar{\theta}_{e,m} = 0$	87	$\bar{\theta}_{e,m} \geq 0$	$87-8.9\bar{\theta}_{e,m}$
2–3	$\bar{\theta}_{e,m} = 0$	550	$\bar{\theta}_{e,m} \geq 0$	$550-29\bar{\theta}_{e,m}$
3–4	$\bar{\theta}_{e,m} = 0$	1030	$\bar{\theta}_{e,m} \geq 0$	$1030-29\bar{\theta}_{e,m}$

Table 1.27 Finland and Estonia, indoor climate, pivots (weekly means).

Indoor climate	Difference in indoor/outdoor vapour pressure (Pa)		
	$\bar{\theta}_{e,w} < 5\,°C$	$5 \leq \bar{\theta}_{e,w} \leq 15\,°C$	$\bar{\theta}_{e,w} > 15\,°C$
Low humidity load	540	$540-34\bar{\theta}_{e,w}$	200
Average humidity load	680	$680-41\bar{\theta}_{e,w}$	270
High humidity load	810	$810-47\bar{\theta}_{e,w}$	340

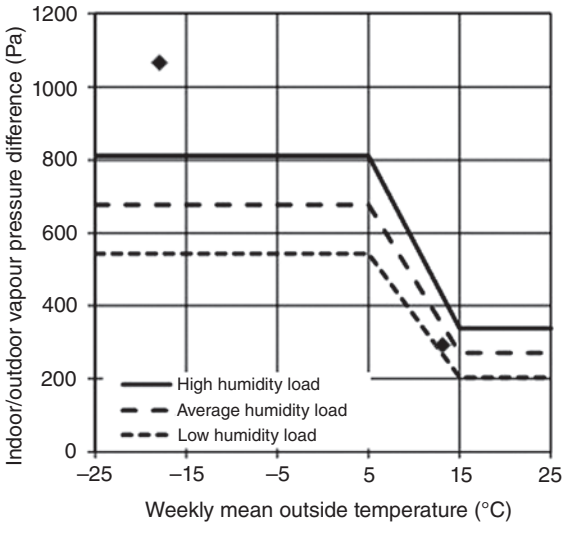

Figure 1.29 Finland and Estonia indoor climate: differences in indoor to outdoor vapour pressure (the two lonely dots represent averages measured in northern Canada).

Table 1.28 EN-ISO 13788, indoor climate classes, pivot values.

Indoor climate classes	Pivot $\Delta\bar{p}_{ie}$ (Pa)	
	$\bar{\theta}_{e,m} < 0$	$\bar{\theta}_{e,m} \geq 0$
1–2	270	$270 - 13.5\ \bar{\theta}_{e,m}$
2–3	540	$540 - 27.0\ \bar{\theta}_{e,m}$
3–4	810	$810 - 40.5\ \bar{\theta}_{e,m}$
4–5	1080	$1080 - 54.0\ \bar{\theta}_{e,m}$

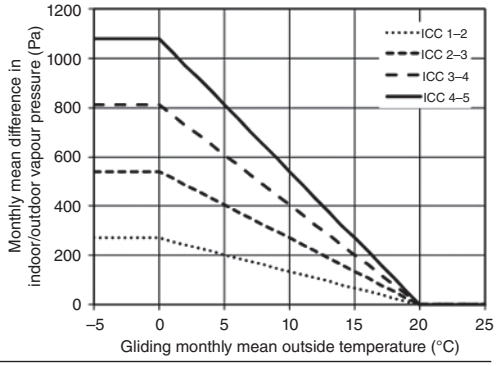

1.3.4 Indoor to Outdoor Air Pressure Differentials

Thermal stack, wind and fans induce air pressure differentials, the driving force causing air in- and exfiltration. Wind additionally favours wind washing, while thermal stack is responsible for indoor air washing and outside air looping in envelope assemblies. With the air, non-negligible amounts of water vapour and enthalpy are displaced, causing thermal transmittances and transient thermal properties to lose significance, interstitial condensation to turn more likely and bulkier, end energy use to increase, draught to emerge and sound insulation to degrade.

In winter, stack gives overpressure indoors. In warm weather, it causes under-pressure indoors each time the temperatures there drop below the value

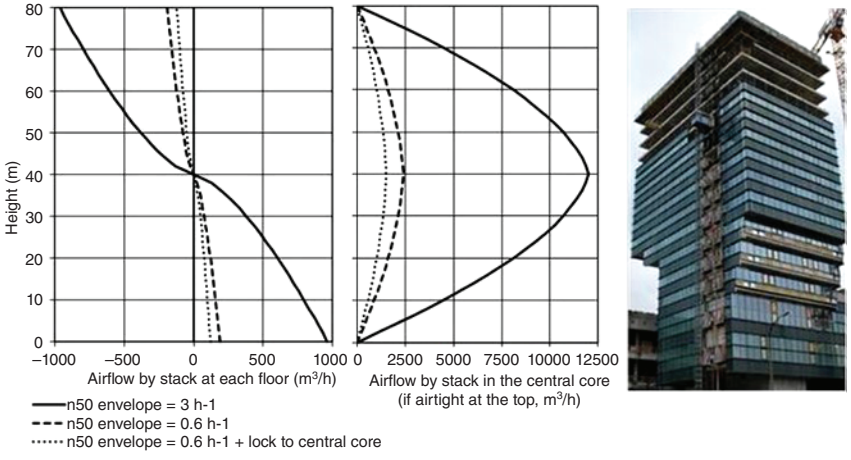

Figure 1.30 Medium rise office building, air flow caused by thermal stack.

outdoors. The pressure differentials that wind induces change with wind velocity and wind direction. They further depend on the pressure coefficients and the leak distribution over the enclosure and the indoors. An enclosure that is most permeable at the windward side will give overpressure indoors with air leaving the building at the leeward side and the sides more or less parallel to the wind direction. The pressures, forced air heating and mechanical ventilation give, differ between spaces. Some industrial buildings experience extreme values. In the supply plenum above the HEPA filter ceiling of a clean room, overpressures up to 150 Pa were measured, while 300 Pa was noted in the top-floor of a hop kiln.

While wind mainly gives ever-changing pressure differentials and while those caused by mechanical ventilation are often small, except in very airtight buildings and some industrial premises, those induced by thermal stack are, though variable, nearly permanently active and can touch high values in high-rises, as do the related in- and outflows. Figure 1.30 illustrates this for a medium-rise office building. Minimisation demands measures such as a really airtight envelope, an airtight lock around the central core and other.

Annex: Solar Radiation at Uccle, Belgium (50° 51′ N, 4° 21′ E)

Table A1 gives the beam radiation on a surface perpendicular to the solar beam under clear sky conditions. Table A2 lists the diffuse solar radiation on a horizontal surface under clear sky conditions. Both consider the 15th of each month. Table A3 compiles beam plus diffuse solar radiation under clear sky conditions for surfaces with different orientation and slope. Table A4 gives the total solar beam and diffuse radiation for each month, while Table A5 gives that total, now included reflected solar radiation.

Table A1 Beam radiation under clear sky conditions on a surface perpendicular to the solar beam for the 15th of each month (W/m^2).

Hour ↓	J	F	M	A	M	J	J	A	S	O	N	D
4.0	0	0	0	0	0	103	45	0	0	0	0	0
4.5	0	0	0	0	133	223	165	0	0	0	0	0
5.0	0	0	0	29	248	321	270	119	0	0	0	0
5.5	0	0	0	169	355	412	370	246	48	0	0	0
6.0	0	0	0	293	445	489	454	356	192	0	0	0
6.5	0	0	138	399	518	552	524	446	314	112	0	0
7.0	0	0	274	484	578	603	580	519	414	251	0	0
7.5	0	163	383	551	625	645	626	577	494	359	153	0
8.0	102	279	469	604	664	680	664	623	555	445	268	97
8.5	218	378	536	646	695	708	694	660	603	510	360	219
9.0	315	455	587	678	719	730	718	689	640	559	430	310
9.5	389	513	626	704	739	749	738	712	668	596	482	379
10.0	445	557	655	723	754	763	754	730	689	623	519	430
10.5	484	587	676	736	765	774	765	743	704	640	544	464
11.0	509	608	689	745	772	781	773	751	713	651	558	485
11.5	523	620	697	749	776	785	778	756	717	654	561	494
12.0	525	623	698	749	775	784	778	756	716	650	556	491
12.5	513	612	693	740	767	776	770	748	706	632	532	468
13.0	483	592	678	728	756	768	761	739	692	609	500	435
13.5	450	569	654	710	739	752	748	723	670	581	460	392
14.0	403	536	629	690	722	736	733	705	646	543	405	333
14.5	338	490	595	664	700	717	714	683	613	492	331	254
15.0	252	428	549	629	673	693	690	655	571	425	236	156
15.5	142	347	490	586	639	664	661	619	217	336	118	0
16.0	0	243	413	531	596	628	625	573	448	229	0	0
16.5	0	80	315	461	544	584	580	517	359	102	0	0
17.0	0	0	196	373	478	530	526	448	250	0	0	0
17.5	0	0	55	265	398	464	459	358	120	0	0	0
18.0	0	0	0	142	302	385	378	252	0	0	0	0
18.5	0	0	0	0	191	291	282	133	0	0	0	0
19.0	0	0	0	0	70	187	175	0	0	0	0	0
19.5	0	0	0	0	0	75	60	0	0	0	0	0

Table A2 Diffuse solar radiation under clear sky conditions on a horizontal surface for the 15th of each month (W/m^2).

Hour ↓	J	F	M	A	M	J	J	A	S	O	N	D
4.0	0	0	0	0	0	20	9	0	0	0	0	0
4.5	0	0	0	0	25	44	32	0	0	0	0	0
5.0	0	0	0	5	48	64	53	22	0	0	0	0
5.5	0	0	0	31	70	84	74	47	8	0	0	0
6.0	0	0	0	55	90	102	93	69	34	0	0	0
6.5	0	0	24	76	107	118	110	89	57	19	0	0
7.0	0	0	48	95	123	133	125	106	78	43	0	0
7.5	0	27	69	111	137	146	139	121	95	63	24	0
8.0	16	47	87	125	149	158	151	134	109	79	43	15
8.5	34	61	101	137	160	168	162	145	122	93	59	34
9.0	51	79	114	147	169	177	171	155	132	104	72	49
9.5	64	91	124	156	177	185	180	164	141	113	82	61
10.0	74	100	132	163	183	192	187	171	147	120	90	70
10.5	81	107	138	168	188	197	192	176	153	124	95	76
11.0	86	112	142	172	192	200	196	180	156	127	98	80
11.5	89	115	144	173	193	202	198	182	157	128	98	82
12.0	89	116	145	173	193	202	198	182	157	127	97	81
12.5	87	113	141	170	190	199	195	180	154	122	93	77
13.0	81	109	139	166	185	195	191	176	149	117	86	71
13.5	75	104	132	160	179	188	186	170	142	110	78	64
14.0	66	96	125	153	172	181	179	163	135	101	68	53
14.5	55	87	116	144	163	173	171	155	125	89	54	40
15.0	40	74	105	133	153	164	162	145	114	76	38	24
15.5	22	59	92	121	142	153	151	134	101	59	19	2
16.0	0	40	75	107	129	141	139	120	85	39	0	0
16.5	0	13	56	90	114	128	126	106	66	17	0	0
17.0	0	0	34	71	98	113	111	89	45	0	0	0
17.5	0	0	9	49	80	97	95	70	21	0	0	0
18.0	0	0	0	26	59	78	76	48	0	0	0	0
18.5	0	0	0	0	37	58	58	25	0	0	0	0
19.0	0	0	0	0	13	37	34	0	0	0	0	0
19.5	0	0	0	0	0	14	11	0	0	0	0	0

Table A3 Solar radiation under clear sky conditions for the 15th of each month (direct and diffuse, W/m^2).

Hour ↓	J	F	M	A	M	J	J	A	S	O	N	D
Horizontal surface												
4.0	0	0	0	0	0	26	8	0	0	0	0	0
4.5	0	0	0	0	36	68	46	0	0	0	0	0
5.0	0	0	0	4	84	122	95	33	0	0	0	0
5.5	0	0	0	50	146	188	157	83	10	0	0	0
6.0	0	0	0	107	219	262	228	147	58	0	0	0
6.5	0	0	37	178	297	338	305	220	117	28	0	0
7.0	0	0	93	256	375	414	381	299	188	79	0	0
7.5	0	37	159	335	451	487	456	376	263	138	34	0
8.0	16	87	230	410	522	559	527	449	337	202	77	16
8.5	54	143	302	479	591	629	597	517	405	265	124	52
9.0	96	201	367	542	656	694	663	582	465	322	171	90
9.5	138	256	424	599	714	748	722	640	518	371	214	128
10.0	176	304	472	647	758	785	766	691	562	410	250	161
10.5	208	342	510	685	787	799	791	730	596	438	276	187
11.0	232	370	537	711	802	798	799	755	618	454	292	205
11.5	245	386	552	724	806	794	799	767	629	460	296	212
12.0	247	391	555	723	805	794	798	768	626	453	290	210
12.5	239	384	545	708	797	799	799	758	610	435	272	197
13.0	220	365	524	680	777	798	794	734	582	406	244	175
13.5	191	335	491	640	742	781	772	698	543	366	207	145
14.0	155	295	448	590	692	741	732	649	485	316	163	109
14.5	115	245	395	533	631	685	676	591	439	258	115	71
15.0	72	190	333	469	564	618	611	527	375	195	69	34
15.5	32	131	264	399	493	548	542	459	304	131	26	0
16.0	0	76	192	323	420	476	470	387	229	73	0	0
16.5	0	28	122	244	344	402	397	311	155	24	0	0
17.0	0	0	62	167	265	327	321	232	89	0	0	0
17.5	0	0	12	98	188	250	244	157	35	0	0	0
18.0	0	0	0	42	119	177	171	92	0	0	0	0
18.5	0	0	0	0	63	113	107	40	0	0	0	0
19.0	0	0	0	0	19	61	55	0	0	0	0	0
19.5	0	0	0	0	0	21	15	0	0	0	0	0

(Continued)

Table A3 Solar radiation under clear sky conditions for the 15th of each month (direct and diffuse, W/m^2). (Continued)

Hour ↓	J	F	M	A	M	J	J	A	S	O	N	D
Vertical surface ($s = 90°$) north ($a_s = 180°$)												
4.0	0	0	0	0	0	83	49	0	0	0	0	0
5.0	0	0	0	22	119	169	144	61	0	0	0	0
6.0	0	0	0	53	120	163	152	89	25	0	0	0
7.0	0	0	29	52	66	82	77	59	43	25	0	0
8.0	6	25	43	57	68	73	71	62	51	39	23	7
9.0	26	38	49	60	68	72	71	64	55	46	35	25
10.0	36	44	53	62	67	71	69	65	58	50	41	34
11.0	40	48	56	62	67	70	69	65	59	52	44	38
12.0	41	49	56	62	67	70	69	65	59	52	44	39
13.0	39	48	55	62	67	70	69	65	59	50	41	36
14.0	34	44	53	61	68	71	70	65	56	46	35	28
15.0	22	37	48	59	68	73	71	64	52	39	22	13
16.0	0	24	40	55	67	74	71	61	46	24	0	0
17.0	0	0	23	47	101	134	113	58	32	0	0	0
18.0	0	0	0	48	131	179	161	90	0	0	0	0
19.0	0	0	0	0	60	128	113	24	0	0	0	0
Tilted surface, slope 60° ($s = 60°$) north ($a_s = 180°$)												
4.0	0	0	0	0	0	82	45	0	0	0	0	0
5.0	0	0	0	21	138	198	164	65	0	0	0	0
6.0	0	0	0	88	198	256	231	138	37	0	0	0
7.0	0	0	39	90	196	254	235	145	59	34	0	0
8.0	8	34	58	81	165	227	208	116	71	53	31	9
9.0	34	50	67	86	129	194	174	94	77	62	46	33
10.0	46	58	73	88	101	162	142	95	81	67	54	44
11.0	51	63	75	89	101	141	121	95	82	69	57	49
12.0	53	64	76	89	101	137	116	95	83	69	57	49
13.0	50	62	75	89	101	151	128	95	81	67	53	46
14.0	43	58	72	87	118	180	154	95	78	62	45	36
15.0	29	49	65	84	155	213	188	94	73	52	28	16
16.0	0	31	55	78	189	244	221	131	63	32	0	0
17.0	0	0	31	96	203	261	239	149	43	0	0	0
18.0	0	0	0	57	163	231	213	115	0	0	0	0
19.0	0	0	0	0	59	135	120	21	0	0	0	0

Table A3 Solar radiation under clear sky conditions for the 15th of each month (direct and diffuse, W/m^2). (Continued)

Hour ↓	J	F	M	A	M	J	J	A	S	O	N	D
Tilted surface, slope 30° (s = 30°) north ($a_s = 180°$)												
4.0	0	0	0	0	0	61	30	0	0	0	0	0
5.0	0	0	0	14	124	180	145	55	0	0	0	0
6.0	0	0	0	108	233	291	258	158	51	0	0	0
7.0	0	0	47	190	319	375	346	246	117	40	0	0
8.0	9	40	91	253	382	439	411	312	172	64	36	10
9.0	39	61	130	300	435	495	466	362	214	78	55	38
10.0	54	72	159	336	472	527	504	401	244	89	64	51
11.0	61	78	176	356	484	521	509	423	261	100	68	57
12.0	62	80	181	360	485	516	506	427	263	99	68	58
13.0	59	77	173	346	478	528	511	416	250	88	63	53
14.0	51	71	152	317	448	513	493	386	224	77	53	42
15.0	33	59	120	275	399	464	445	342	185	63	33	19
16.0	0	37	80	219	340	404	381	286	133	38	0	0
17.0	0	0	36	144	262	330	314	211	70	0	0	0
18.0	0	0	0	55	158	230	215	115	0	0	0	0
19.0	0	0	0	0	44	110	98	12	0	0	0	0
Vertical surface (s = 90°) east ($a_s = 90°$)												
4.0	0	0	0	0	0	117	70	0	0	0	0	0
5.0	0	0	0	82	228	353	300	156	0	0	0	0
6.0	0	0	0	366	532	562	529	428	243	0	0	0
7.0	0	0	335	582	652	654	645	608	492	287	0	0
8.0	116	293	517	634	648	646	648	640	582	444	245	111
9.0	247	401	527	566	566	568	577	572	529	441	313	221
10.0	257	361	418	425	417	417	435	437	393	327	256	217
11.0	168	228	248	236	222	225	245	251	211	160	128	127
12.0	54	68	78	83	86	88	89	87	78	66	54	48
13.0	44	55	64	69	72	74	75	72	65	55	44	39
14.0	35	46	54	60	64	66	66	63	56	47	35	29
15.0	22	37	47	54	58	60	60	57	49	38	22	13
16.0	0	23	38	46	52	54	54	50	41	22	0	0
17.0	0	0	21	36	44	47	47	42	27	0	0	0
18.0	0	0	0	16	31	38	37	27	0	0	0	0
19.0	0	0	0	0	8	21	20	0	0	0	0	0

(Continued)

Table A3 Solar radiation under clear sky conditions for the 15th of each month (direct and diffuse, W/m^2). (Continued)

Hour ↓	J	F	M	A	M	J	J	A	S	O	N	D
Tilted surface, slope 60° ($s = 60°$) east ($a_s = 90°$)												
4.0	0	0	0	0	0	112	64	0	0	0	0	0
5.0	0	0	0	73	285	358	300	149	0	0	0	0
6.0	0	0	0	364	560	606	562	435	234	0	0	0
7.0	0	0	329	621	739	760	736	664	510	281	0	0
8.0	106	291	552	740	807	823	809	764	660	475	244	103
9.0	255	437	626	745	801	820	813	769	676	530	346	229
10.0	300	451	582	672	718	731	738	703	603	472	334	258
11.0	248	366	462	534	565	566	585	569	468	344	240	199
12.0	138	225	296	353	386	397	412	391	292	182	107	93
13.0	60	78	114	157	199	232	241	200	107	77	61	53
14.0	46	63	76	86	93	98	98	92	79	63	47	38
15.0	29	49	62	73	80	84	84	78	66	49	28	16
16.0	0	30	48	61	68	73	73	66	53	29	0	0
17.0	0	0	26	46	56	62	61	54	34	0	0	0
18.0	0	0	0	20	40	48	48	35	0	0	0	0
19.0	0	0	0	0	10	27	25	0	0	0	0	0
Tilted surface, slope 30° ($s = 30°$) east ($a_s = 90°$)												
4.0	0	0	0	0	0	78	41	0	0	0	0	0
5.0	0	0	0	44	209	273	224	103	0	0	0	0
6.0	0	0	0	268	444	485	450	331	166	0	0	0
7.0	0	0	240	500	636	670	638	549	397	204	0	0
8.0	69	214	446	657	760	790	764	693	569	385	182	68
9.0	198	363	566	735	832	865	844	771	651	485	294	181
10.0	269	429	600	752	843	865	858	795	663	501	330	236
11.0	270	416	567	708	778	776	788	753	616	451	299	226
12.0	214	345	479	607	673	673	685	656	517	354	219	166
13.0	124	236	352	466	546	577	580	522	380	228	115	82
14.0	56	111	207	306	387	439	437	363	229	95	56	45
15.0	34	59	78	150	227	279	277	205	85	59	32	19
16.0	0	34	57	74	88	137	134	84	63	33	0	0
17.0	0	0	29	53	68	76	75	64	38	0	0	0
18.0	0	0	0	23	46	57	56	39	0	0	0	0
19.0	0	0	0	0	12	31	29	0	0	0	0	0

Table A3 Solar radiation under clear sky conditions for the 15th of each month (direct and diffuse, W/m^2). (Continued)

Hour ↓	J	F	M	A	M	J	J	A	S	O	N	D
Vertical surface (s = 90°) south (a_s = 0°)												
4.0	0	0	0	0	0	11	4	0	0	0	0	0
5.0	0	0	0	2	28	34	30	14	0	0	0	0
6.0	0	0	0	37	50	52	49	42	33	0	0	0
7.0	0	0	111	139	102	72	70	107	157	137	0	0
8.0	91	195	289	291	238	191	192	246	322	331	217	100
9.0	290	402	466	436	370	316	320	384	473	510	418	293
10.0	471	572	602	555	475	411	423	500	590	635	569	462
11.0	585	675	686	627	527	448	472	570	658	698	644	557
12.0	615	707	709	640	532	451	479	585	667	696	640	568
13.0	561	668	669	592	496	434	460	547	614	630	558	493
14.0	426	558	571	491	405	363	388	455	509	502	401	339
15.0	233	382	422	355	278	245	270	327	366	320	198	145
16.0	0	174	239	202	141	117	139	186	204	128	0	0
17.0	0	0	73	64	156	160	161	57	59	0	0	0
18.0	0	0	0	18	35	42	42	31	0	0	0	0
19.0	0	0	0	0	8	22	20	0	0	0	0	0
Tilted surface, slope 60° (s = 60°) south (a_s = 0°)												
4.0	0	0	0	0	0	15	5	0	0	0	0	0
5.0	0	0	0	3	37	45	40	19	0	0	0	0
6.0	0	0	0	63	84	75	68	62	50	0	0	0
7.0	0	0	134	232	255	238	223	223	217	151	0	0
8.0	85	205	353	440	445	421	406	418	432	376	220	93
9.0	292	439	573	631	627	598	586	604	626	590	438	293
10.0	487	636	743	786	770	726	728	759	775	741	607	471
11.0	612	757	847	881	836	765	787	851	863	817	692	575
12.0	646	795	876	898	843	765	793	871	874	815	688	587
13.0	586	749	826	835	798	753	773	821	806	735	594	505
14.0	438	619	703	702	675	662	680	698	772	580	419	341
15.0	232	416	518	524	501	498	517	527	489	364	200	139
16.0	0	183	291	320	311	315	333	335	274	140	0	0
17.0	0	0	87	124	129	139	154	146	86	0	0	0
18.0	0	0	0	24	47	57	57	42	0	0	0	0
19.0	0	0	0	0	11	29	27	0	0	0	0	0

(Continued)

Table A3 Solar radiation under clear sky conditions for the 15th of each month (direct and diffuse, W/m^2). (Continued)

Hour ↓	J	F	M	A	M	J	J	A	S	O	N	D
Tilted surface, slope 30° ($s = 30°$) south ($a_s = 0°$)												
4.0	0	0	0	0	0	17	5	0	0	0	0	0
5.0	0	0	0	3	44	54	47	22	0	0	0	0
6.0	0	0	0	92	165	183	158	113	59	0	0	0
7.0	0	0	126	274	354	365	338	293	227	129	0	0
8.0	57	165	331	482	549	555	529	492	436	328	168	62
9.0	220	364	536	669	731	735	711	675	622	520	347	217
10.0	378	536	694	819	873	862	852	828	764	657	489	360
11.0	481	644	791	910	936	893	906	918	847	727	562	445
12.0	510	678	818	927	942	890	909	937	857	725	558	454
13.0	459	636	771	866	900	886	895	889	793	651	478	387
14.0	338	521	657	737	779	800	805	768	666	511	331	256
15.0	172	344	484	565	605	634	641	600	491	317	152	98
16.0	0	146	273	363	412	446	453	408	284	119	0	0
17.0	0	0	83	161	218	258	263	210	96	0	0	0
18.0	0	0	0	27	65	96	99	58	0	0	0	0
19.0	0	0	0	0	13	34	32	0	0	0	0	0
Vertical surface ($s = 90°$) west ($a_s = -90°$)												
4.0	0	0	0	0	0	11	4	0	0	0	0	0
5.0	0	0	0	2	26	32	28	13	0	0	0	0
6.0	0	0	0	29	41	44	42	35	20	0	0	0
7.0	0	0	27	43	50	52	50	46	38	24	0	0
8.0	6	25	40	51	56	58	57	53	47	38	23	7
9.0	26	38	49	57	62	63	62	59	54	47	36	26
10.0	37	47	56	65	69	70	69	67	63	56	45	37
11.0	47	56	67	76	81	82	80	77	74	67	55	46
12.0	75	77	106	148	162	145	130	134	157	169	141	98
13.0	100	244	297	349	362	336	323	334	347	335	265	201
14.0	266	370	455	514	529	512	500	502	499	445	312	230
15.0	222	397	539	615	631	621	613	610	579	440	231	147
16.0	0	274	485	623	661	661	657	641	535	274	0	0
17.0	0	0	262	476	583	616	614	550	321	0	0	0
18.0	0	0	0	198	368	453	447	315	0	0	0	0
19.0	0	0	0	0	109	211	200	57	0	0	0	0

Table A3 Solar radiation under clear sky conditions for the 15th of each month (direct and diffuse, W/m^2). (Continued)

Hour ↓	J	F	M	A	M	J	J	A	S	O	N	D
Tilted surface, slope 60° (s = 60°) west ($a_s = -90°$)												
4.0	0	0	0	0	0	14	5	0	0	0	0	0
5.0	0	0	0	2	33	41	36	17	0	0	0	0
6.0	0	0	0	37	52	57	54	44	26	0	0	0
7.0	0	0	34	55	65	68	66	59	49	31	0	0
8.0	8	32	53	67	76	79	77	71	62	50	30	9
9.0	35	50	66	80	89	92	89	83	75	64	48	34
10.0	50	64	80	96	144	158	133	99	91	78	62	49
11.0	64	82	163	270	331	329	310	281	241	191	120	65
12.0	72	241	343	461	513	492	480	470	423	352	251	175
13.0	270	377	499	621	649	666	652	633	571	477	339	250
14.0	298	455	602	722	785	794	779	740	663	530	342	246
15.0	222	429	620	753	812	830	819	776	676	468	229	141
16.0	0	269	506	689	769	796	790	736	567	268	0	0
17.0	0	0	252	486	626	685	680	582	316	0	0	0
18.0	0	0	0	188	370	471	463	311	0	0	0	0
19.0	0	0	0	0	102	208	196	49	0	0	0	0
Tilted surface, slope 30° (s = 30°) west ($a_s = -90°$)												
4.0	0	0	0	0	0	16	5	0	0	0	0	0
5.0	0	0	0	3	38	47	41	19	0	0	0	0
6.0	0	0	0	42	62	68	64	51	29	0	0	0
7.0	0	0	38	66	81	87	83	72	57	35	0	0
8.0	9	37	63	91	183	216	188	123	78	60	35	10
9.0	41	61	101	238	338	371	340	270	188	101	58	40
10.0	61	123	246	399	501	524	499	432	339	235	125	61
11.0	151	248	389	551	639	635	625	583	482	360	228	147
12.0	234	355	507	672	749	730	726	702	594	455	304	215
13.0	276	421	581	741	830	835	824	779	656	502	330	239
14.0	257	426	598	749	843	877	863	793	660	482	286	201
15.0	167	351	543	698	786	828	817	744	599	377	169	99
16.0	0	196	397	577	679	726	720	641	453	193	0	0
17.0	0	0	178	371	508	577	571	464	230	0	0	0
18.0	0	0	0	130	278	369	361	229	0	0	0	0
19.0	0	0	0	0	69	152	142	28	0	0	0	0

Table A4 Beam and diffuse solar radiation under permanent clear sky conditions (MJ/(m^2 mo)).

Surface ↓	J	F	M	A	M	J	J	A	S	O	N	D
Hor.	136	232	424	610	787	823	825	705	497	324	168	111
North												
$s = 30°$	42	59	150	352	564	643	627	461	236	82	48	36
$s = 60°$	35	48	77	120	236	330	301	171	90	63	41	31
$s = 90°$	28	37	56	81	134	170	161	105	64	47	31	24
E+W												
$s = 30°$	136	226	406	572	731	761	764	659	471	313	167	113
$s = 60°$	129	207	359	484	604	623	627	552	408	281	156	109
$s = 90°$	102	159	268	345	419	428	768	388	297	213	122	88
South												
$s = 30°$	292	410	618	742	844	829	849	801	660	521	334	252
$s = 60°$	377	489	662	695	708	656	686	709	663	591	419	333
$s = 90°$	365	442	538	479	415	352	380	450	500	511	396	327
SE+SW												
$s = 30°$	242	353	554	695	817	817	832	765	605	457	282	209
$s = 60°$	292	392	564	641	700	673	695	679	586	487	329	258
$s = 90°$	268	336	444	456	459	422	442	464	440	401	295	242
NE+NW												
$s = 30°$	52	106	245	422	611	674	663	521	317	167	68	42
$s = 60°$	40	69	177	270	405	456	446	340	201	106	49	34
$s = 90°$	29	49	104	175	259	294	287	220	133	73	36	26

Table A5 Beam, diffuse and reflected solar radiation under permanent clear sky conditions (MJ/(m^2 mo), albedo 0.2).

Surface ↓	J	F	M	A	M	J	J	A	S	O	N	D
Hor.	136	232	424	610	787	823	825	705	497	324	168	111
North												
$s = 30°$	43	62	156	360	574	654	638	470	242	86	50	37
$s = 60°$	42	60	98	150	276	371	342	206	115	79	49	36
$s = 90°$	41	60	99	142	213	252	243	176	114	80	48	35

Table A5 Beam, diffuse and reflected solar radiation under permanent clear sky conditions (MJ/(m^2 mo), albedo 0.2). (Continued)

Surface ↓	J	F	M	A	M	J	J	A	S	O	N	D
E+W												
$s = 30°$	138	229	412	580	741	772	775	668	478	317	169	115
$s = 60°$	135	218	380	515	644	664	669	587	433	297	164	115
$s = 90°$	116	182	310	406	498	510	515	459	347	245	139	99
South												
$s = 30°$	294	414	624	750	854	840	860	811	667	526	337	254
$s = 60°$	384	500	683	725	747	697	728	744	688	608	427	338
$s = 90°$	379	465	580	540	494	434	463	521	550	544	413	338
SE+SW												
$s = 30°$	244	356	560	703	828	828	843	774	612	461	284	210
$s = 60°$	299	404	585	671	740	714	736	714	611	503	338	263
$s = 90°$	283	360	487	517	537	504	525	534	490	433	312	253
NE+NW												
$s = 30°$	54	110	251	430	622	685	674	531	323	172	71	43
$s = 60°$	46	81	176	300	444	497	487	375	226	122	57	39
$s = 90°$	43	73	146	236	338	376	369	291	182	106	53	37

Further Reading

Anon (1983). *Draft European Passive Solar Handbook*, Section 2 on Climate. CEC.

Antretter, F., Holm, A, Karagiozis, A., and Glass, S. (2010). Interior temperature and relative humidity distributions in mixed-humid and cold climates as building simulation boundary conditions, *Proceedings of the Buildings XI Conference, Clearwater Beach (CD-ROM)*.

Arena, L., Karagiosis, A, and Mantha, P. (2010). Monitoring of internal moisture loads in residential buildings-research findings in three different climate zones, *Proceedings of the Buildings XI Conference, Clearwater Beach (CD-ROM)*.

ASHRAE (2021a). Chapter 14, Climatic design information. In: *Handbook Fundamentals*, 14.1–14.19+tables. ASHRAE.

ASHRAE (2021b). Chapter 37, Moisture management in buildings. In: *Handbook Fundamentals*, 37.1–37.14. ASHRAE.

Berdahl, P. and Fromberg, R. (1982). The thermal radiance of clear skies. *Solar Energy* 29 (4): 299–314.

Best, A.C. (1950). The size distribution of rain drops. *Quarterly Journal of the Royal Meteorological Society* 76: 16–36.

Blocken, B. (2004). Wind-driven rain on buildings, measurement. Numerical modelling and applications, PhD-thesis, K.U.Leuven, 323 p.

Blocken, B., Carmeliet, J., and Hens, H. (1999). Preliminary results on estimating wind driven rain loads on building envelopes: A numerical and experimental approach, K.U.Leuven, Laboratory of Building Physics, 78 p.

Blocken, B., Carmeliet, J., and Hens, H. (2000). On the use of microclimatic data for estimating driving rain on buildings, *Proceedings of the International Building Physics Conference*, TU/e, 581–588.

BRE (1971). An index of exposure to driving rain, digest 127.

CD with weather data from K.U. Leuven, Laboratory of Building Physics, 1996–2008.

Cornick, S. and Rousseau, M. (2003). *Understanding the Severity of Climate Loads for Moisture-related Design of Walls*. IRC Building Science Insight, 13 p.

Cornick, S., Djebbar, R., and Dalgliesh, W. (2003). Selecting moisture reference years using a moisture index approach, IRC Research Paper, 19 p.

Costrop, D. (1985). The use of climate data for simulating of thermal systems, Rapport KU-Leuven-RD-Energie (in Dutch).

Davies, J. and Mc, K.D. (1982). Estimating solar irradiance and components. *Solar Energy* 29 (1): 55–64.

Dogniaux, R. (1978). Recueil des données climatologiques exigentielles pour le calcul des gains solaires dans l'habitat et l'estimation de la consommation de l' énergie pour le chauffage des bâtiments, K.M.I. (Contract EG) (in French).

EN ISO 13788 (2001). Hygrothermal performance of building components and building elements-Internal surface temperature to avoid critical surface humidity and interstitial condensation, calculation method.

EN ISO 15927 (2002). Hygrothermal performance of buildings. Calculation and presentation of climatic data.

Flemish Government (2006). Energy Performance Decree, Text and Addenda (in Dutch).

Geving, S. and Holme, J. (2012). Mean and diurnal indoor air humidity loads in residential buildings. *Journal of Building Physics* 35 (2): 392–421.

Hartmann, T., Reichel, D, and Richter, W. (2001). Feuchteabgabe in Wohnungen – alles gesagt? Gesundheits-Ingenieur 122, H. 4, S. 189–195 (in German).

Hens, H. (1975). Theoretical and experimental study of the hygrothermal behaviour of building- and insulating materials by interstitial condensation and drying, with application on low-sloped roofs, doctoraal proefschrift, KULeuven (in Dutch).

IEA-Annex 14 (1991). Condensation and energy, Sourcebook, Acco Leuven.

ISO (1980). Climatologie et industrie du bâtiment, Rapport, Genève (in French).

Kalamees, T., Vinha, J., and Kurnitski, J. (2006). Indoor humidity loads in light-weight timber-framed detached houses. *Journal of Building Physics* 29 (3): 219–246.

Kumaran, K. and Sanders, C. (2008). Boundary conditions and whole building HAM analysis, Final report IEA-ECBCS Annex 41 'Whole Building Heat, Air, Moisture Response', Volume 3, ACCO, Leuven 235 p.

Künzel, H.M. (2010). Indoor Relative Humidity in Residential Buildings – A Necessary Boundary Condition to Assess the Moisture Performance of Building Envelope Systems.

Künzel, H.M., Zirkelbach, D., and Sedlbauer, K. (2003). Predicting Indoor Temperature and Humidity Conditions Including Hygrothermal Interactions with the Building

Envelope, *Proceedings of the First Intenational Conference on Sustainable Energy and Green Architecture, Bangkok, 8–10 October 2003*.

Laverge, J., Delgust, M., and Janssens, A. (2014). Moisture in bathrooms and kitchens: the impact of ventilation, *Proceedings of NSB 2014 Lund*, 998–1005 (data stick).

Liddament, M.W. (1986). Air infiltration calculation techniques, AIVC.

Poncelet, L. and Martin, H. (1947). Main characteristics of the Belgian climate, Verhandelingen van het K.M.I. (in Dutch).

Ridley, I., Davies, M., Hong, S. H., and Oreszcyn, T. (2008). Vapour pressure excess in living rooms and bedrooms of English dwellings: analysis of the warm front dataset, Appendix III of the IEA-ECBCS Annex 41 report on 'Boundary Conditions and Whole Building HAM Analysis', ACCO Leuven, 187–205.

Sanders, C. (1996). Environmental Conditions, Final report IEA-ECBCS Annex 24 'Heat, Air and Moisture Transfer in Insulated Envelope Parts', Volume 2, ACCO, Leuven, 96 p.

Straube, J. (1998). Moisture control and enclosure wall systems, PhD-thesis, University of Waterloo (Canada).

Straube, J. and Burnett, E. (2000). Simplified prediction of driving rain on buildings, *Proceedings of the International Building Physics Conference*, TU/e, 375–382.

Ten Wolde, A. and Pilon, C. (2007). The effect of indoor humidity on water vapor release in homes, *Proceedings of the Buildings X Conference, Clearwater Beach (CD-ROM)*.

Uyttenbroeck, J. (1985). Exterior climate data for energy consumption and load calculations, Rapport WTCB-RD-Energie (in Dutch).

Uyttenbroeck, J. en Carpentier G., (1985). Exterior climate data for building physics applications, Rapport WTCB-RD-Energie (in Dutch).

Vaes, F. (1984). Hygrothermal behaviour of light-weight ventilated roofs, onderzoek IWONL-KULeuven-TCHN, eindrapport (in Dutch).

Van Mook, F. (2002). Driving rain on building envelopes, PhD-thesis, TU/e, 198 p.

Wouters, P., L'Heureux, D., and Voordecker, P., 1987, The wind as parameter in ventilation studies, a short description, rapport WTCB (in Dutch).

WTCB (1969). Study of the heat gains by natural illumination of buildings, part 1, Solar irradiation. *Researchrapport* 10: (in Dutch).

WTCB tijdschrift (1982). Moisture response of building components, 1 (52 p.) (in Dutch and in French).

Ernst & Sohn
A Wiley Brand

Georgios Gaganelis, Peter Mark, Patrick Forman

Optimization Aided Design

Reinforced Concrete

- **numerous examples e.g. columns, beams, deep beams, corbels, cantilevers, frame corners, pylons, parabolic trough solar collectors, fiber reinforced concrete**
- **the book is suitable for graduates, young professionals and for teaching & research**
- **useful introduction to optimization methods for practicing engineers**

Reinforced concrete is the dominating building material and contributes to resource consumption and climate change. The book provides design methods for minimal material use in its outer and inner shape. Numerous examples illustrate the application in theory and practice.

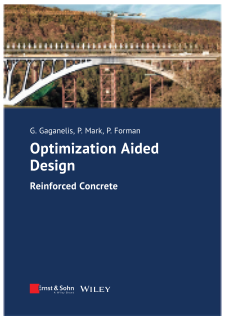

2022 · 184 pages · 200 figures · 6 tables

Softcover
ISBN 978-3-433-03337-1 **€ 69***

eBundle (Softcover + ePDF)
ISBN 978-3-433-03338-8 **€ 99***

ORDER
+49 (0)30 470 31-236
marketing@ernst-und-sohn.de
www.ernst-und-sohn.de/en/3337

* All book prices inclusive VAT.